ARMY RESEARCH LABORATORY

Mechanical Alloying Effects in Ball-Milled Tungsten-Copper (W-Cu) Composites

by Laszlo J. Kecskes, Matthew D. Trexler, Bradley R. Klotz, Kyu C. Cho, and Robert J. Dowding

ARL-TR-2465 April 2001

The findings in this report are not to be construed as an official Department of the Army position unless so designated by other authorized documents.

Citation of manufacturer's or trade names does not constitute an official endorsement or approval of the use thereof.

Destroy this report when it is no longer needed. Do not return it to the originator.

Army Research Laboratory
Aberdeen Proving Ground, MD 21005-5069

ARL-TR-2465 **April 2001**

Mechanical Alloying Effects in Ball-Milled Tungsten-Copper (W-Cu) Composites

Laszlo J. Kecskes, Matthew D. Trexler, Bradley R. Klotz,
Kyu C. Cho, and Robert J. Dowding
Weapons and Materials Research Directorate, ARL

Abstract

Fine-grained, high-density (97%+ of theoretical density [TD]), 80 tungsten-20 copper weight-percent (80W-20Cu [58W-42Cu atomic-percent]) composites have been prepared using nonconventional alloying techniques. The W and Cu precursor powders were combined by high-energy ball milling in air. A second set of W+Cu mixtures was prepared in hexane to reduce contamination of the powders. The mechanically alloyed W+Cu powder mixtures were then coldpressed into green compacts and sintered at 1,250 °C. The effects of varying the milling medium and milling time were examined with density measurements. Longer milling increased product densities with a concomitant order-of-magnitude decrease in grain size; air was found to be a more effective medium than hexane. Residual impurities were identified with energy-dispersive x-ray spectroscopy (EDS), and their effects on sample properties were evaluated with microhardness measurements. X-ray diffraction (XRD) and scanning electron microscopy (SEM) analyses demonstrated that the as-milled W-Cu alloy structures were metastable, decomposing into the starting W and Cu components upon heating at or above 450 °C.

Acknowledgments

The authors gratefully note the contributions of Mr. Daniel Snoha for his careful review of the manuscript and his comments regarding the determination and sources of ball-milling-induced lattice strain.

INTENTIONALLY LEFT BLANK.

Contents

INTENTIONALLY LEFT BLANK.

List of Figures

INTENTIONALLY LEFT BLANK.

List of Tables

INTENTIONALLY LEFT BLANK.

1. Introduction

Tungsten-heavy alloys (WHAs) are continually being investigated for both commercial and military applications. Most WHAs consist of W particles embedded in a matrix of other metals such as iron (Fe), nickel (Ni), or copper (Cu) [1]. W-Cu composites may have potential uses as heat dissipation materials in the microelectronics field [2], divertor plates in fusion reactors [3], or as warhead materials for military ordnance applications. It has been postulated that if high-density W could be combined with ductile Cu, the resultant W-Cu composite may be a more suitable material for shaped charge liners.

The alloying of W and Cu proves to be difficult due to the mutual insolubility of W and Cu. The assessed equilibrium phase diagram [4] in Figure 1 reveals that the two metals are completely immiscible in both solid and liquid phases. This limitation excludes the use of conventional alloying techniques to develop full density W-Cu alloys.

Several alternate processing techniques have been examined to develop W-Cu composites [5]. Most commonly, W-Cu is alloyed through the sintering of finely divided W-Cu powder mixtures. Both solid-state- and liquid-phase-sintering (SSS and LPS) techniques can be used depending on the composite and its desired characteristics. SSS of W-Cu may be performed at any temperature, but LPS of W-Cu requires a sintering temperature that is at least higher than the melting point of Cu (T_m = 1,085 °C). In some cases, when mechanical alloying is used, LPS may occur at lower temperatures. Specifically, as the powder particle size is reduced through welding and fracture during milling [6, 7], the powder structure is often refined to nanoscale. As a result, diffusion paths are decreased, which in turn, reduces the required temperature [8].

The objective of this effort was to intimately mix W and Cu precursors using mechanical alloying and then sinter the resultant mixture into near-full-density, disk-shaped W-Cu pellets. The effect of the milling time and the type of medium used on the development of the composite microstructure was of primary concern. Powder mixtures of 80W-20Cu weight-percent (58W-42Cu atomic-percent) were ball milled in air or hexane for varying times ranging from 0 min to 48 hr (2,880 min). The milled powder mixtures were then cold-pressed into green compacts and sintered into dense pellets. The samples were examined with x-ray diffraction analysis (XRD), scanning electron microscopy (SEM), energy dispersive x-ray spectroscopy (EDS), and Vickers microhardness measurements. Density measurements of the pellets were used to verify if lengthening the milling time resulted in higher product densities. XRD was used

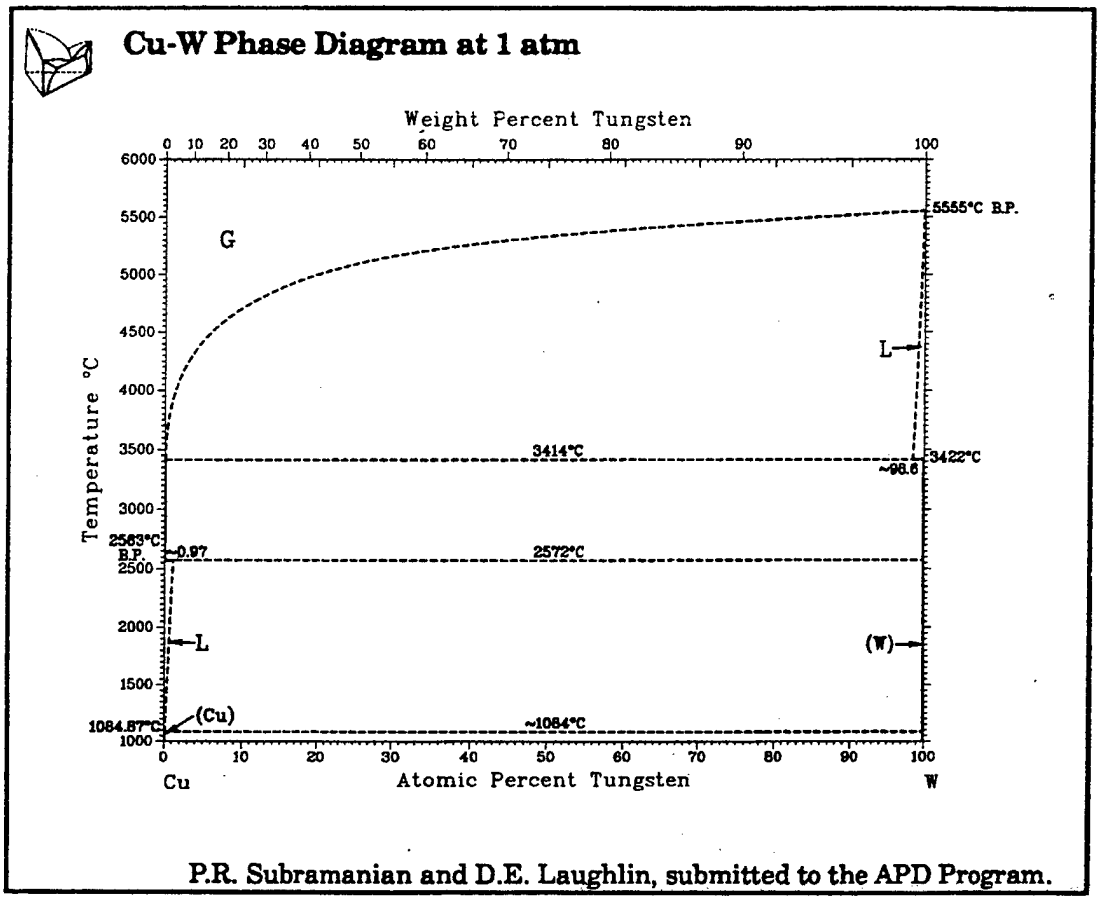

Figure 1. Equilibrium phase diagram of the W-Cu system at 1 atm.

to discern the extent of mechanical alloying and to determine the lattice spacing of the major phases. The precursor and product microstructures were examined by SEM to verify the particle size reduction, redistribution, and intermixing of the two initial phases. The presence and relative amounts of the elemental constituents and alloyed phases were confirmed with EDS. Since, typically, ball milling was expected to add impurities to the powders with increasing milling time, EDS was also used to quantify the impurities that possibly contaminated the powders during the milling process. Finally, Vickers microhardness measurements were performed and correlated to the residual porosity, average grain size, and excess impurity levels in the product structures.

2. Experimental Description

W* (99.9%, 4–4.5 μm) and Cu† (99%, –325 mesh [–44 μm]) powders were weighed, then mixed in air in a Turbula 500 shaker-mixer‡ for 30 min to produce an 80W-20Cu weight-percent powder blend. The blended mixture was placed in steel jars and milled in a Model 8000-D SPEX mill§ for times ranging from 0 min to 48 hr (2,880 min), using two 3.2-mm-diameter and four 1.6-mm-diameter steel balls. The powder-to-ball ratio was maintained at 1:1 by weight. After the milling had been completed, approximately 10 g of powder from each mixture was cold pressed into 12.5-mm-diameter and 10-mm-thick green compacts at a pressure of 300 MPa. The powders were not heat treated since the increased lattice strain was believed to enhance sinterability. The density of each green compact was determined by a direct measurement of the pellet dimensions prior to sintering. The remainder of the milled powder was saved for XRD, SEM, and EDS analyses.

The sintering schedule and environment were selected based on previous works involving both SSS and LPS of W-Cu composites [8, 9]. The green compacts were liquid-phase sintered in hydrogen (flow rate of 20 standard L/min) for 30 min at a temperature of 1,250 °C. The densities of the sintered pellets were determined using Archimedes' Principle. After sintering, the pellets were sectioned with a diamond saw. Pieces, both in transverse and longitudinal orientations with respect to the pellet axis, were mounted in Bakelite and metallographically prepared for SEM and EDS. Specifically, the samples were sequentially diamond polished to a 1/4-μm finish. During polishing, the softer Cu phase tended to smear onto the harder W phase. As a result, a final polish with SiO_2 in an alkaline solution was used to remove the excess Cu material. Additionally, care had to be maintained to prevent oxidation of the freshly prepared Cu-phase surface. A canned, standardless, semi-quantitative EDS analysis routine, available from KEVEX SpectraTrace,** was used to quantify the major phase compositions and to detect residual impurities. Microhardness tests were performed with a 200-g-load Vickers indenter. At least 20 individual hardness measurements were made on each sample. The typical limit of error on the hardness values was about ±0.15 GPa.

* OSRAM Sylvania, Towanda, PA.

† Johnson Matthey, Ward Hill, MA.

‡ Glenn Mills, Clifton, NJ.

§ SPEX CertiPrep., Metuchen, NJ.

** Noran Instruments, Middleton, WI.

The mechanically alloyed powders and cross sections from the sintered pellets were examined using XRD with monochromatic CuKα radiation. The intensity vs. Bragg angle data for all XRD samples were collected from a 2θ of 20 to 120° with a 0.025° step size and 5-s dwell time. The intercept method was used to obtain the lattice parameters of the W and Cu phases [10]. Using 6 or 7 Bragg peaks over the scanned angle range, the approximate limit of error in the lattice parameter measurements was estimated to be ±0.0002 nm. However, for Cu, with very long milling times (i.e., longer than 480 min), only 2–4 peaks could be detected, due to extensive peak broadening. As a result, errors in these Cu lattice parameters were considerably higher (±0.0005 nm or more). The XRD scans were also used to identify the relative amounts of the major phases and to verify the extent of alloying in forming new W-Cu phase. The peak intensities of the W(110), 2θ of 40.3°, and Cu(111), 2θ of 43.3°, are most intense in the XRD pattern. However, due to peak broadening at extreme milling times these peaks tend to overlap. Therefore, the Cu(200), 2θ of 50.4°, and W(200), 2θ of 58.2°, peaks were analyzed instead. The Cu and W peak widths at half maximum were measured and the peaks integrated for both the precursor and sintered samples to monitor relative changes, if any, with respect to milling time.

Based on the results obtained from the first series of 80W-20Cu samples (referred to as "series A" hereafter), two additional series of samples were prepared. Because data for series A were incomplete (Table 1), a second series of samples was prepared in air (series B). Additionally, a third series of 80W-20Cu samples was prepared in hexane (series C). For series B, the preparation procedures were identical to those used for series A. For series C, the ball-milling portion of the preparation sequence was performed under hexane to limit the extent of oxidation. Note that in the series B and C samples, one of the smaller steel balls was removed to slightly change the powder-to-ball mass ratio to 1.05:1.

Finally, in an auxiliary experiment (referred to as "series D" hereafter), about 100 g of 80W-20Cu powder was ball milled for 8 hr in air. Prior to the nominal sintering schedule, 10-g to 12-g batches from the master blend were annealed in hydrogen at temperatures ranging from 350–1,050 °C for 60 min. A small amount from each batch was retained for XRD analysis, while the rest of the powder batch was pressed into a compact and sintered at 1,250 °C. A comparison as a function of temperature of the annealed powder and sintered pellet was intended to examine and differentiate the effects of size-attrition- and ball-milling-induced lattice strain. These experiments also served to determine the optimum temperature at which milling induced strain was mostly removed, but serious grain growth did not take place.

3. Results and Discussion

3.1 Densification Results

Table 1 displays the milling time, green and sintered densities, and microhardness of the samples. The densities were normalized to the theoretical density (TD) of 80W-20Cu, 15.64 gcm^{-3}. As evidenced by the data in Table 1 and Figure 2, both milling time and medium significantly affected densification of the samples. The compaction of finer precursors did not result in higher green densities. Sintered densities were relatively low for milling times shorter than 240 min for samples from series A and B (i.e., those milled in air). Beyond 240 min, the density reached a maximum of about 98% TD, after which it declined. It is speculated that, at longer milling times, oxide build-up on the ultrafine, highly reactive powder surfaces may inhibit sintering. No density data was taken for series A beyond 480 min. Samples from series C took considerably longer to reach near-full density. Most likely, the use of hexane kept the particles suspended in liquid, whereby the effectiveness of the ball-milling action was retarded. In fact, within the milling times examined, the decrease in the density observed in the air-milled samples could not be confirmed. Further experiments are needed to verify this phenomenon by extending the milling times well beyond 2,880 min (e.g., 5,760 min or longer). Alternatively, densification may improve, as suggested by Upadhyaya and German [9], if smaller amounts of powders are milled using much lower powder-to-ball mass ratios.

3.2 Microstructural Characteristics

SEM was performed on the as-milled powders and sintered pellets from all three series. Consistent with the manufacturer's specification for the precursor powders, the W powder was made up of polyhedral particles, ranging in size from 2–5 μm, that form multiparticle aggregates. In contrast, the Cu powder was considerably larger, consisting of rounded, polycrystalline 10-μm to 50-μm particles. As such, the as-mixed powder blend was significantly mismatched at the onset of milling.

Backscatter electron micrographs (BEMs) in Figure 3 delineate the effect of milling in air for the series A powders. In Figures 3(a)–3(h), representative samples are shown from the as-mixed powder and 15-, 30-, 120-, 240-, 480-, 1,440- and 2,880-min milling times. In the BEM, the lighter W and darker Cu particles are easily recognized. Between 0 and 30 min, the finer W grains first adhere to the larger Cu grains. With longer times, the W grains, still adhering to the Cu grains, become deformed (i.e., flattened) into 0.2-μm to 1-μm-thick, rounded

Table 1. Densification results for the W-Cu ball-milled samples.

Sample	Milling Time (min)	Green Density (% TD)	Sinter Density (% TD)	Microhardness 200 gf (GPa)
Series A; Mixed in Air				
A1	0	77.7	81.8	1.87
A2	15	77.9	80.0	1.82
A3	30	78.2	82.0	1.87
A4	60	79.8	89.9	1.86
A5	120	80.2	93.0	2.17
A6	240	77.7	96.9	3.16
A7	480	75.7	85.3	2.92
A8	1,440	–	–	3.51
A9	2,880	–	–	4.39
Series B; Mixed in Air				
B1	120	78.8	89.4	2.04
B2	240	78.9	94.4	2.65
B3	480	73.6	97.8	3.59
B4	480	75.8	97.9	3.57
B5	1,440	67.2	97.5	3.80
B6	2,880	66.5	92.5	3.69
Series C; Mixed in Hexane				
C1	120	76.7	88.1	1.93
C2	240	75.8	86.1	2.07
C3	240	73.0	87.7	2.23
C4	480	72.9	86.7	2.47
C5	480	72.6	90.4	2.39
C6	1,440	70.3	94.9	4.12
C7	2,880	66.9	97.6	3.28

flakes with very high thickness-to-diameter aspect ratios. Between 120 and 480 min, the large W-Cu aggregates become compositionally more homogeneous as the W particles continue to break down into smaller 0.2-μm to 0.5-μm fragments. Thus, with milling, the initial size mismatch is only eliminated after approximately 480 min. Note how the atomic number contrast present in Figures 3(a)–3(d) diminishes in Figures 3(e) and 3(f). The large-sized W-Cu aggregates typically consist of submicrometer-sized W grain fragments coated with a thin layer of Cu. Beyond 1,440 min (Figures 3[g] and 3[h]), aside from the continued attrition of the W-Cu aggregate size, no significant changes occur in the particle morphology.

The examination of the milled powders from series C showed that hexane primarily retarded the attrition of W and delayed the intermixing of W and Cu. Figure 4 depicts the side-by-side evolution of the milled series B and C powders.

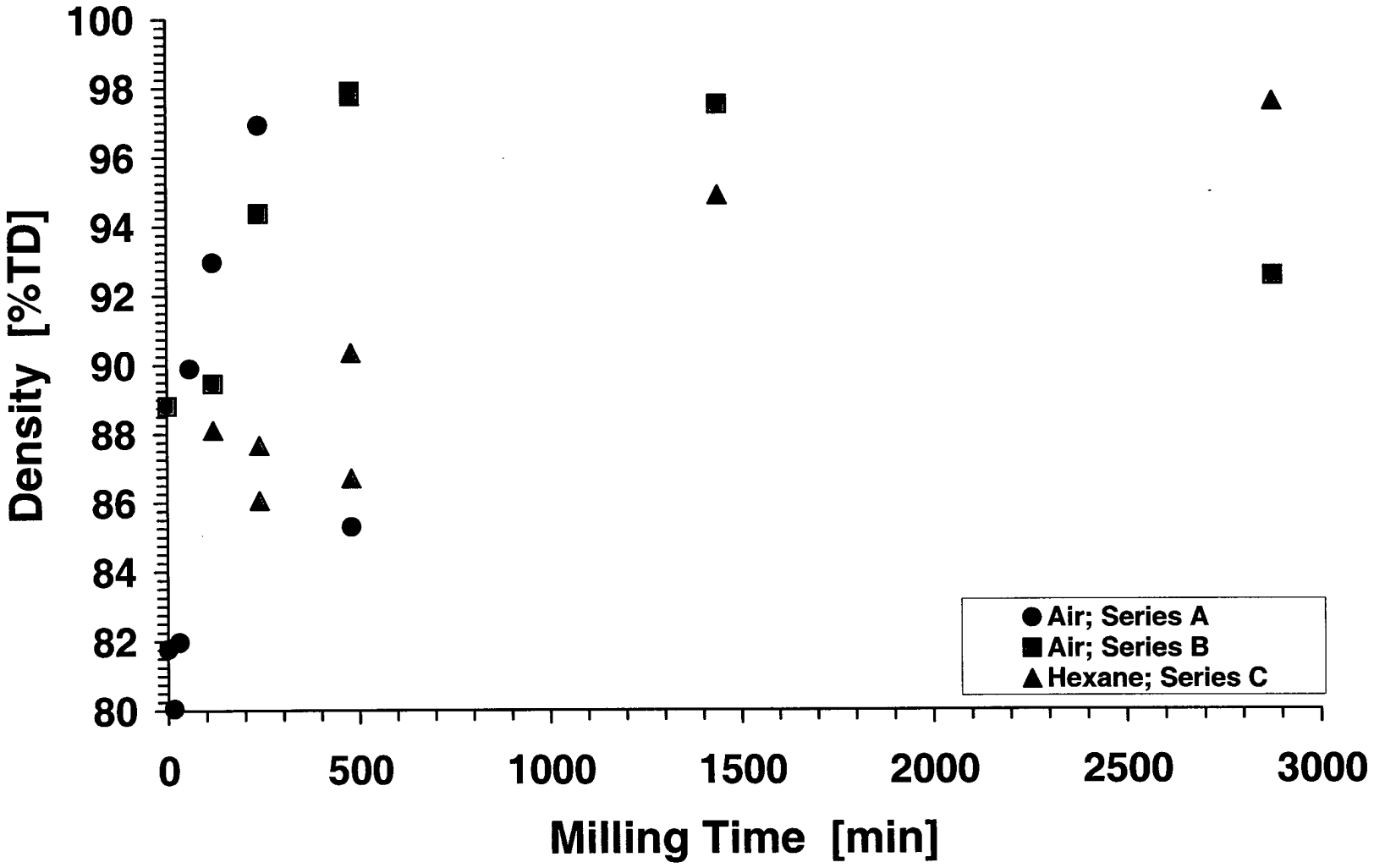

Figure 2. Densification as a function of milling time.

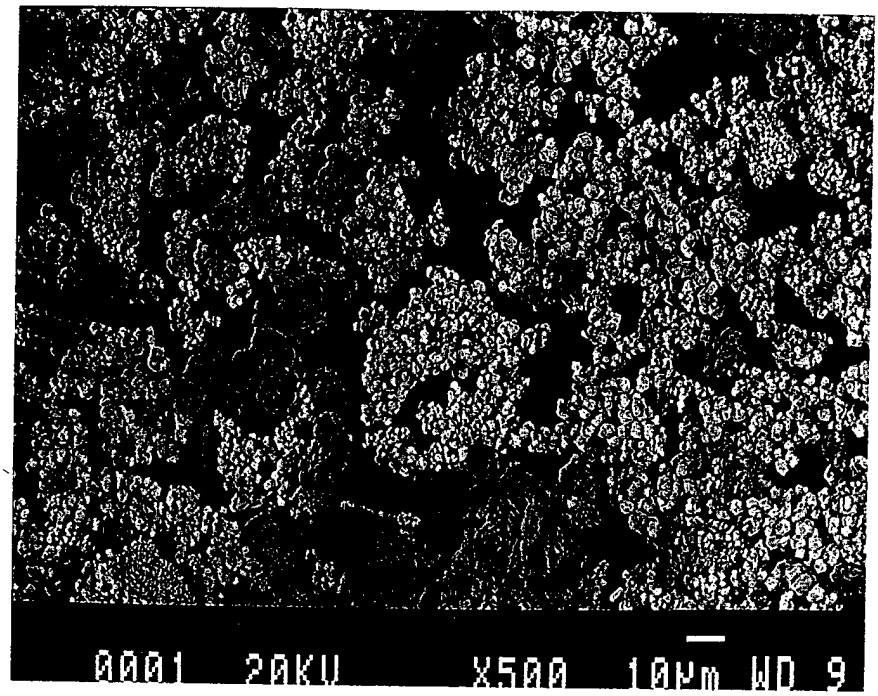

(a) as mixed

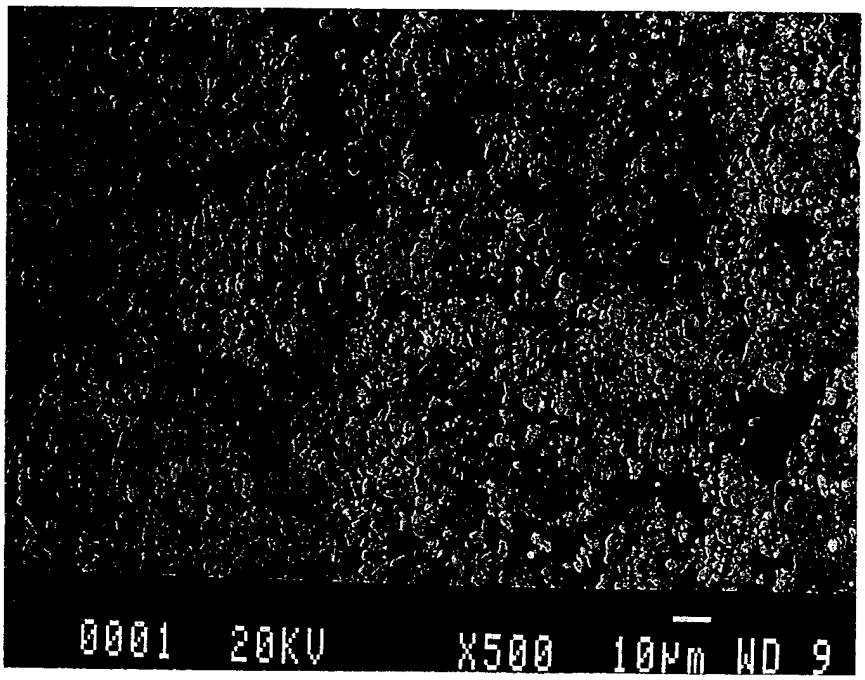

(b) 15 min

Figure 3. BEMs of the as-milled powders.

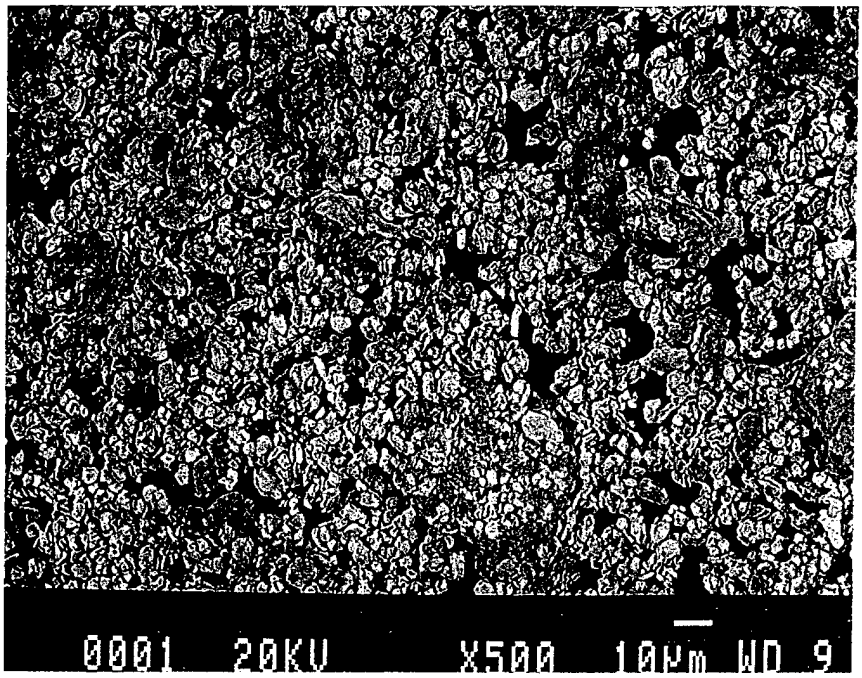

(c) 30 min

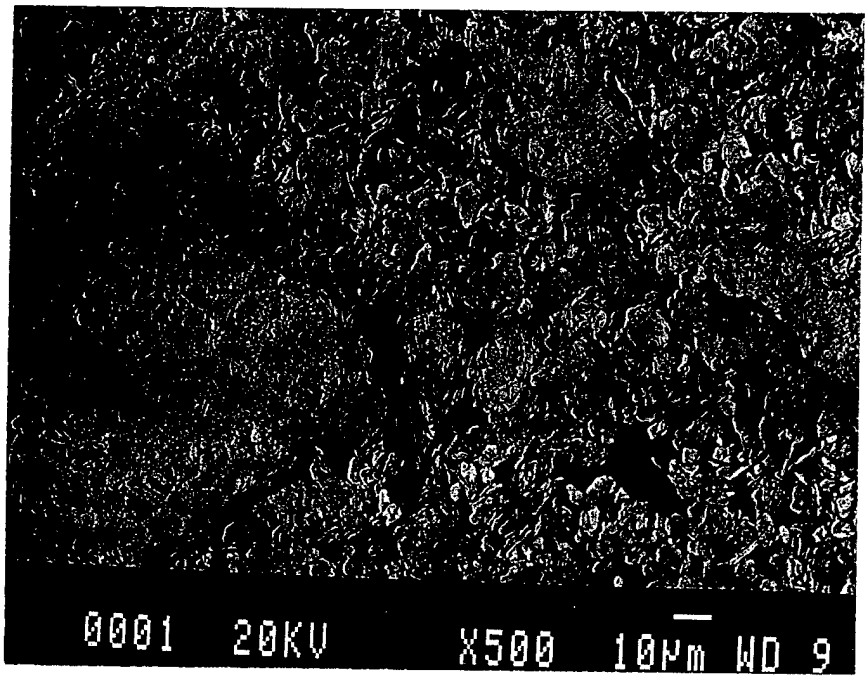

(d) 120 min

Figure 3. BEMs of the as-milled powders (continued).

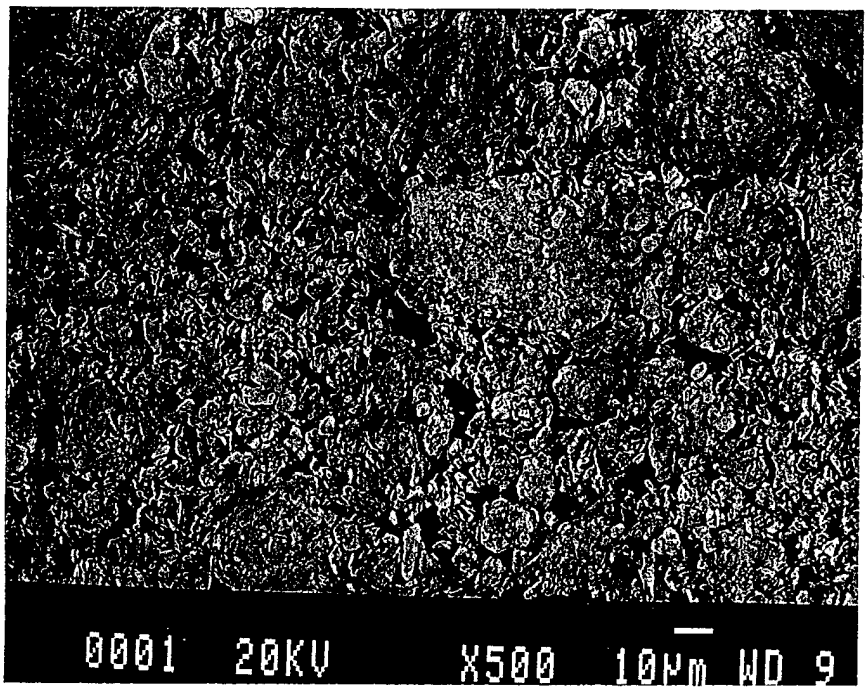

(e) 240 min

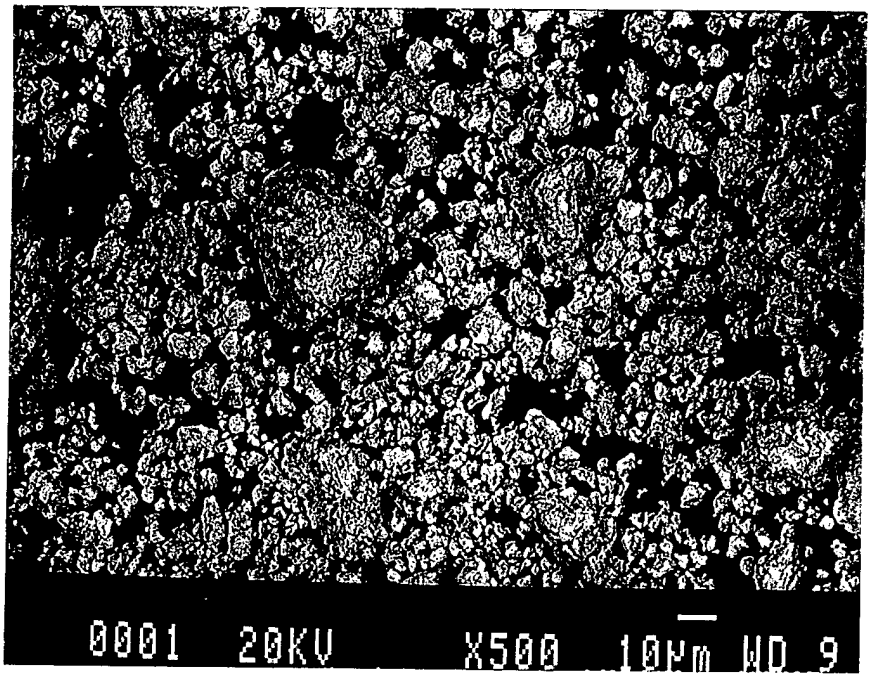

(f) 480 min

Figure 3. BEMs of the as-milled powders (continued).

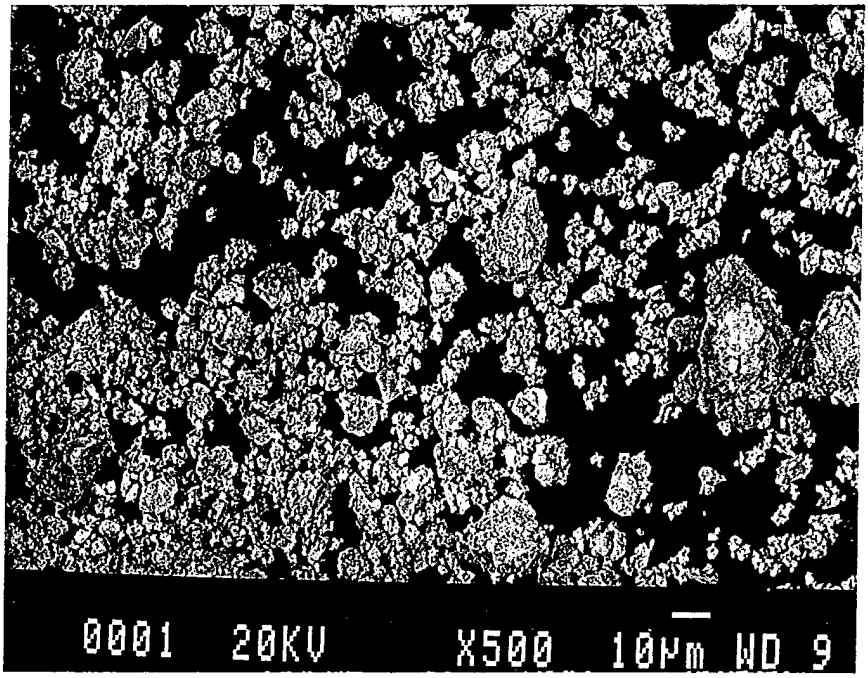

(g) 1,400 min

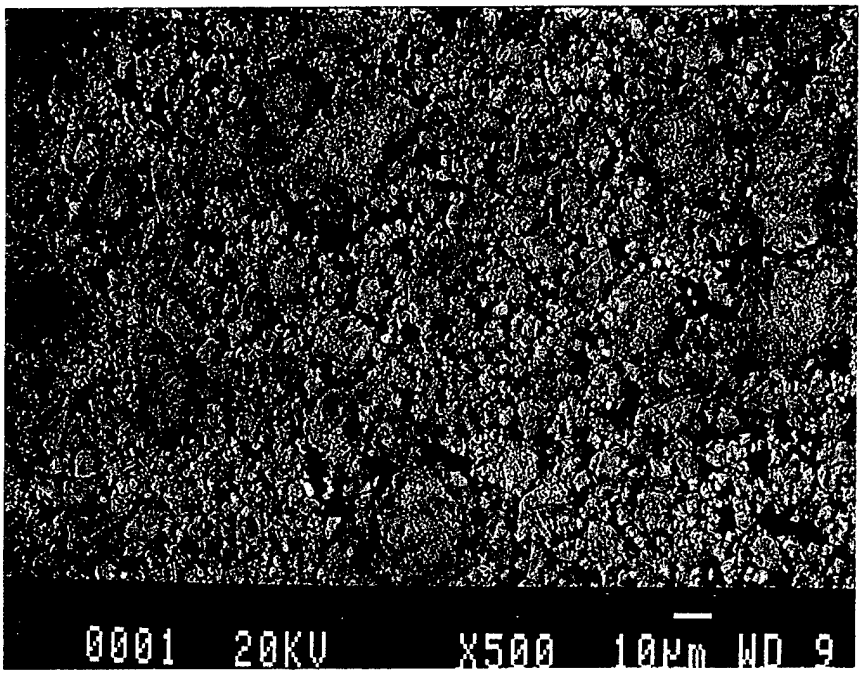

(h) 2,440 min

Figure 3. BEMs of the as-milled powders (continued).

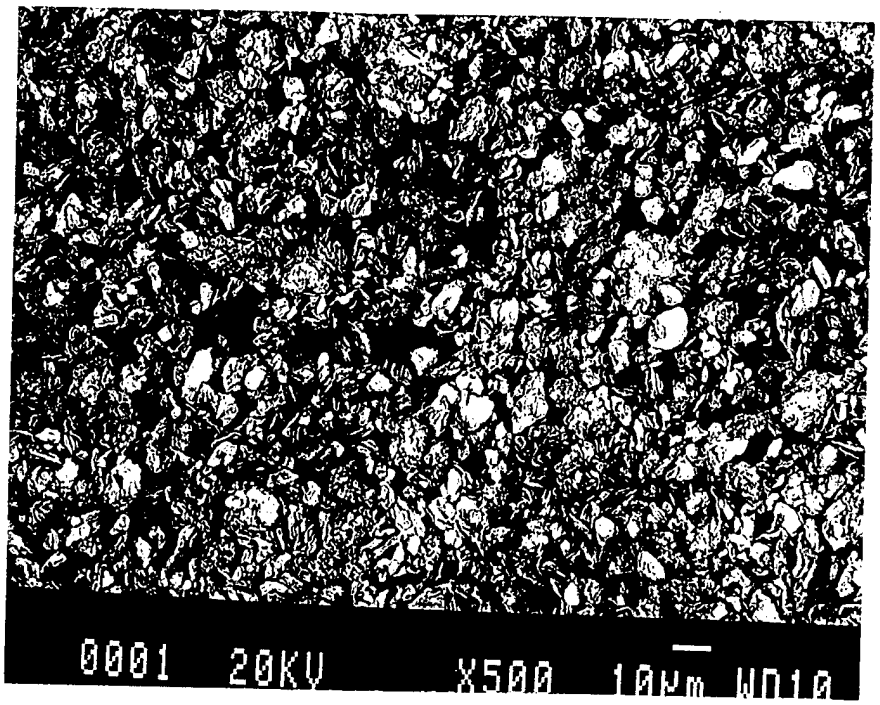

(a) air-milled 240 min

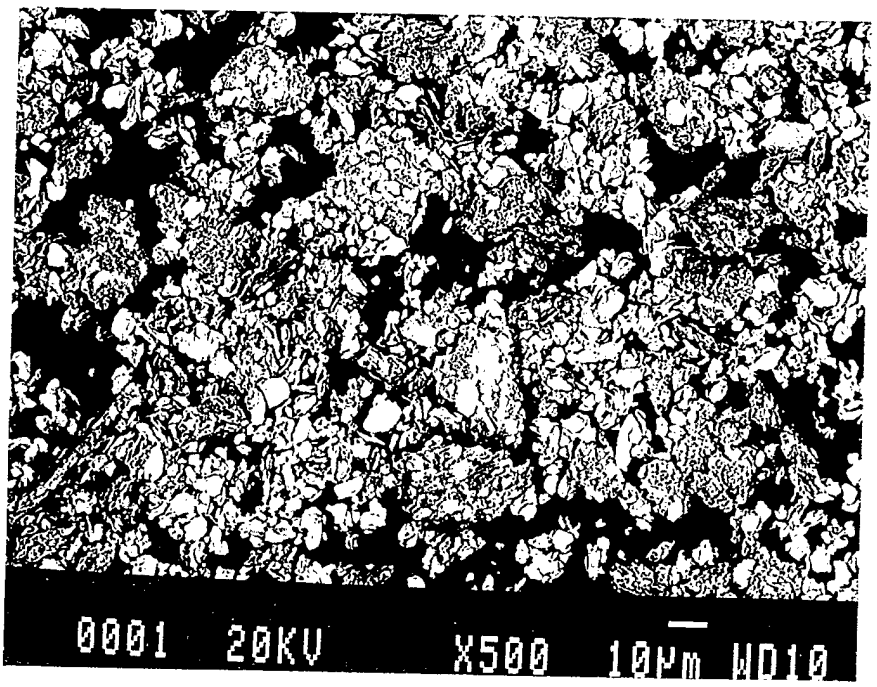

(b) hexane-milled 240 min

Figure 4. Comparative BEMs of the as-milled powders in hexane and air.

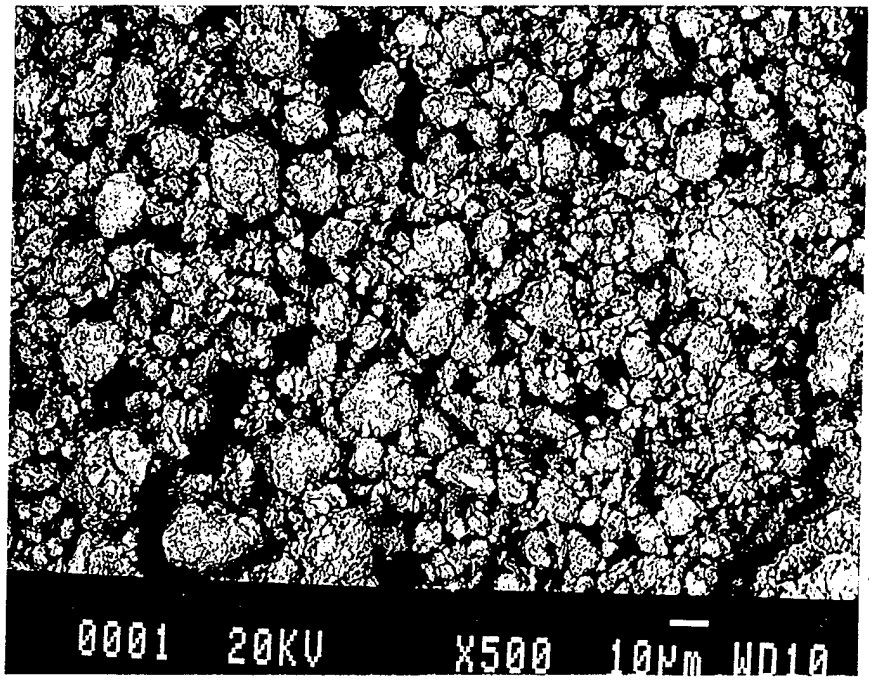

(c) air-milled 480 min

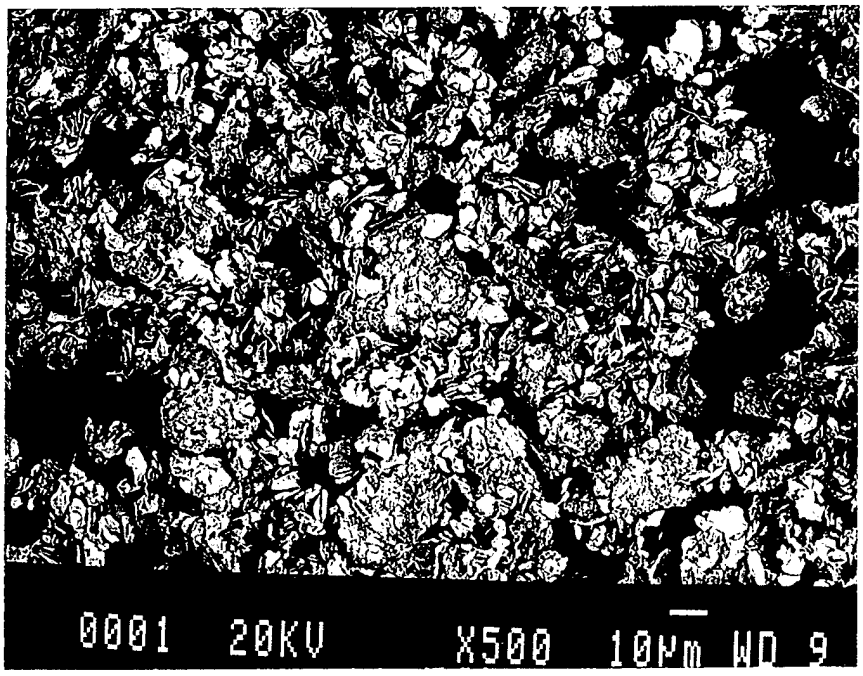

(d) hexane-milled 480 min

Figure 4. Comparative BEMs of the as-milled powders in hexane and air (continued).

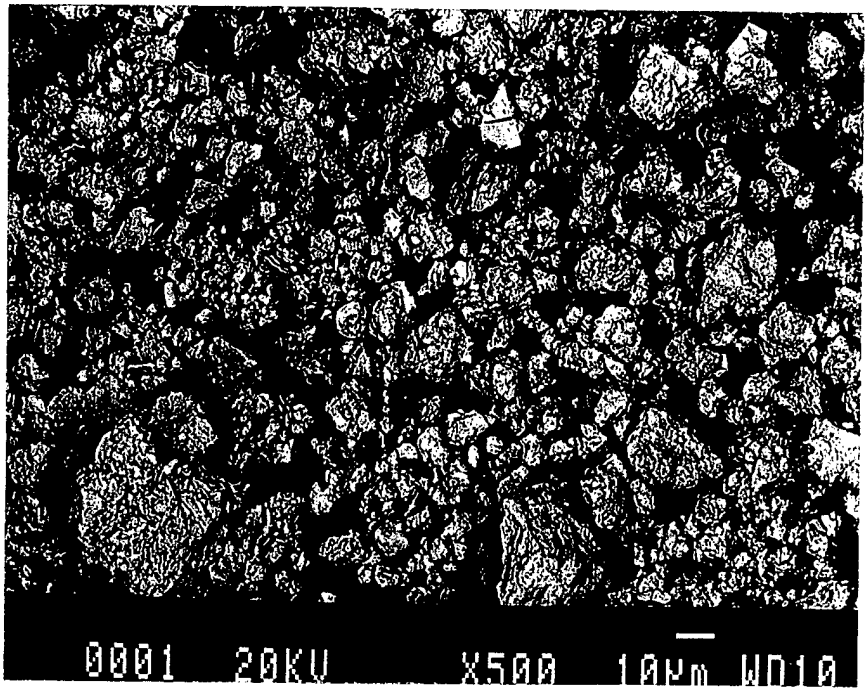

(e) air-milled 1,440 min

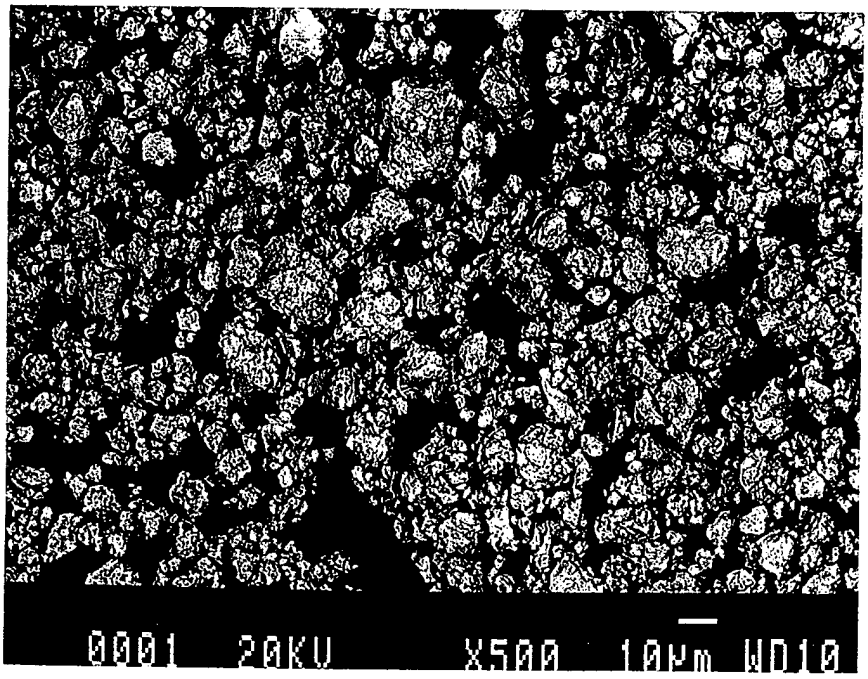

(f) hexane-milled 1,440 min

Figure 4. Comparative BEMs of the as-milled powders in hexane and air (continued).

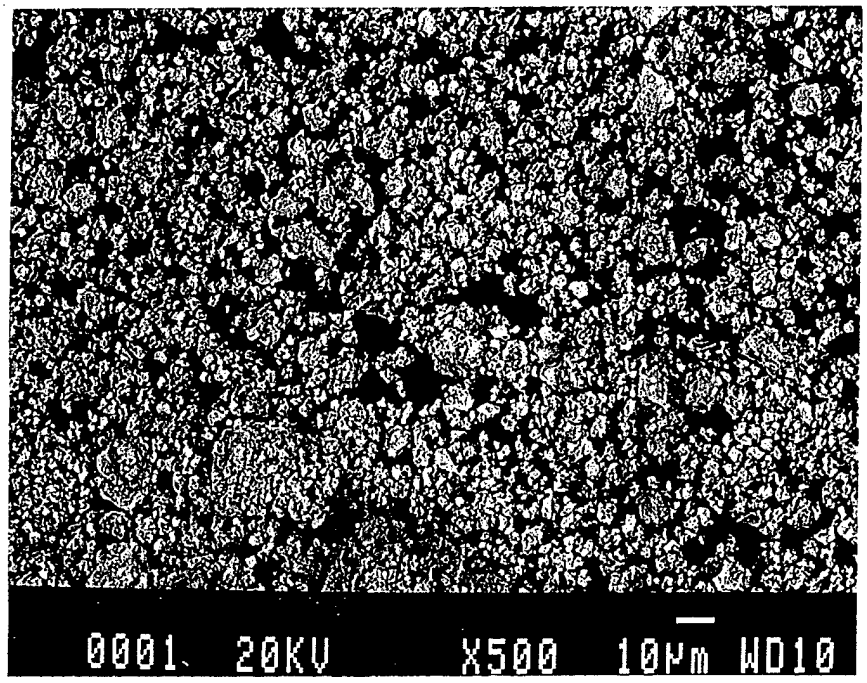

(g) air-milled 2,880 min

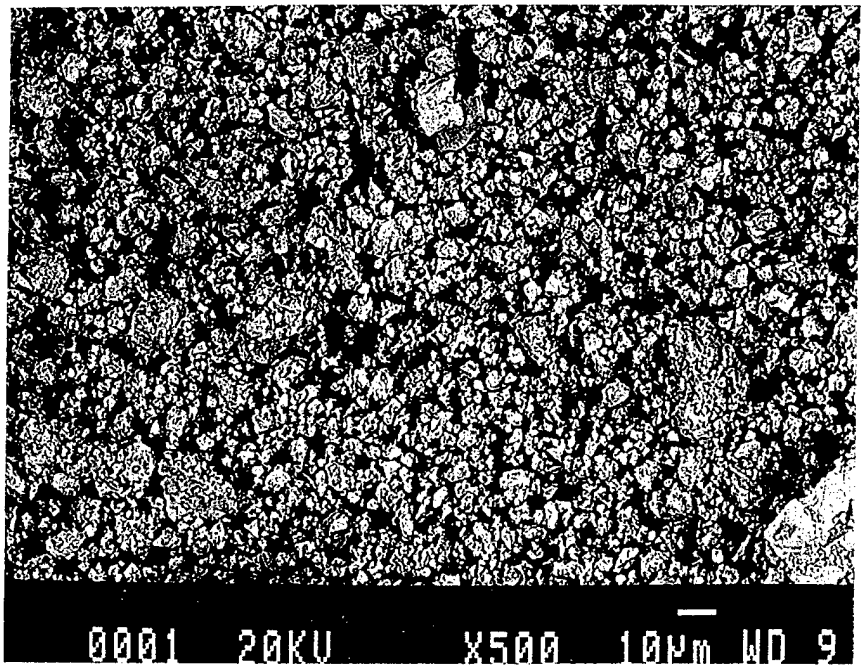

(h) hexane-milled 2,880 min

Figure 4. Comparative BEMs of the as-milled powders in hexane and air (continued).

At 240 min (Figures 4[a] and 4[b]), the W-Cu powder aggregates in hexane appear considerably larger than those milled in air. At 480 min (Figures 4[c] and 4[d]), most of the air-milled W-Cu aggregates appear homogeneous, but the hexane-milled W-Cu aggregates continue to retain platelike W grains. However, these differences are transitory, as at 1,440 min (Figures 4[d] and 4[f]) and beyond (Figures 4[g] and 4[h]), such differences are no longer present.

In both mixes, the powders appeared homogeneous and the W-Cu aggregate sizes were similar.

Recall that it was at about 240–480 min where densification reached near-full density for the air-milled samples. While it may be thought that the use of hexane was in vain, it must be kept in mind that a powder milled in hexane for extended time may not be subjected to as much oxidation as would the powder milled in air.

SEM of longitudinal and transverse cross sections from the series A pellets indicated no noticeable sagging or orientation effect. Figure 5 displays BEMs of representative areas from the as-mixed powder and 15-, 30-, 120-, 240-, 480-, 1,440-, and 2,880-min sintered pellets. As apparent in the figures, the sintered W and Cu morphologies correlate well with those of the milled powders. The micrographs reveal that the darker-colored Cu phase surrounds the lighter-colored (deformed or broken down) W grains. The microstructures of the sintered pellets show a definite improvement in the homogeneity of the composite. It is quite obvious that as milling time increases, the ball-milling-induced work hardening of W causes the grains to fragment, thereby facilitating the rapid intermixing of the two phases at a micrometer level. An average W grain size of about 0.2–0.5 μm was achieved within 480 min of milling. With milling beyond 480 min, the uniformly fine structure begins to coarsen and the residual porosity increases. The increased closed porosity may account for the observed decrease in sample densities. Based on the coarsening in the samples, it is apparent that extended milling improved the sinterability of the powders. SEM of the sintered pellets from series B were consistent with those from series A. In series C, much like the aforementioned densification, the overall structural grain refinement was delayed. SEM of these sintered pellets indicated no new microstructures with increasing milling times.

As major constituents, EDS detected only Cu and W in all three series. The W and Cu phases in the 0- to 30-min samples were mostly pure. At longer milling times, due to the fine-grained structure of the samples, EDS could not be used to verify the anticipated redistribution of the W- or Cu-rich phases. In addition to W and Cu, small amounts of Fe, oxygen, and carbon were detected in most of the samples. Over the span of 2–2,880 min, Fe was found to increase linearly with milling time. In hexane, the amount of Fe pick-up was slightly less than that in air. The Fe contamination was most likely caused by erosion of the steel jar

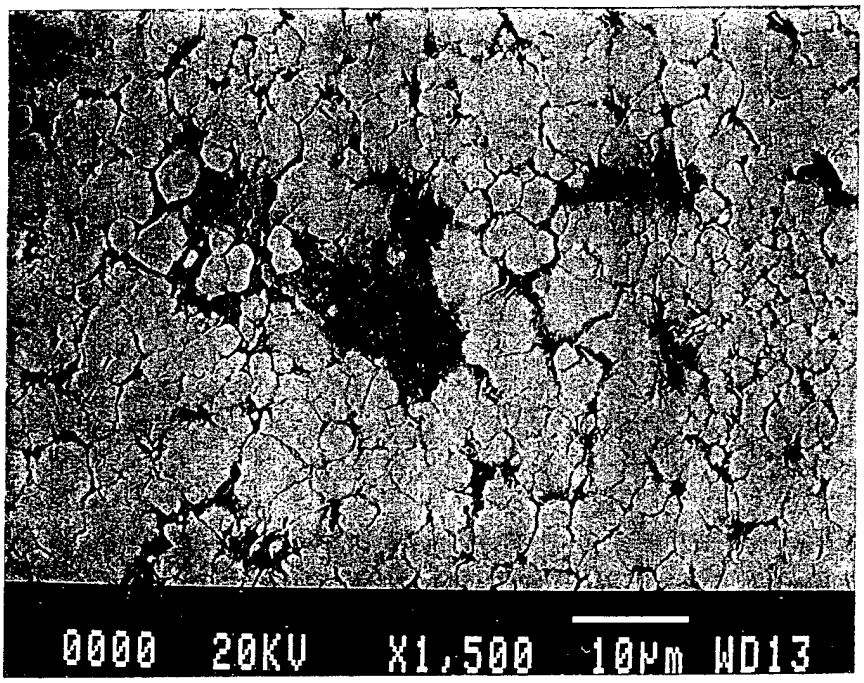

(a) as-mixed powder

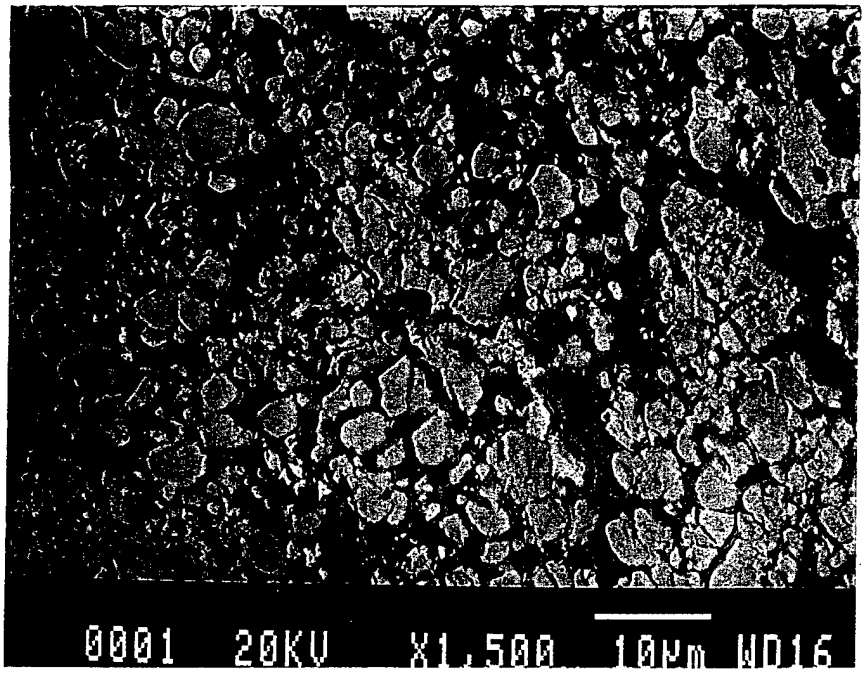

(b) 15-min powder

Figure 5. BEMs of sintered pellets.

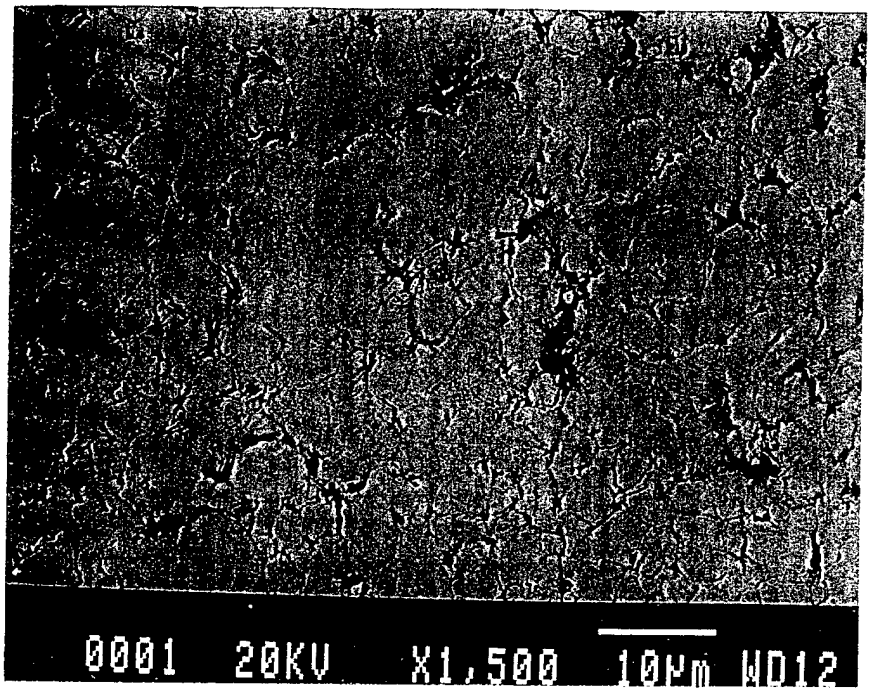

(c) 30-min powder

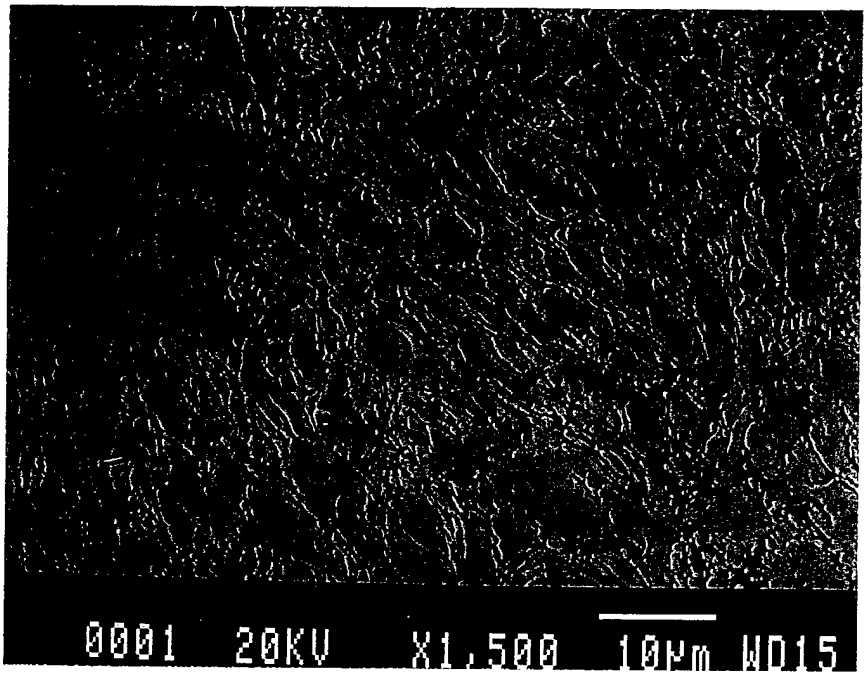

(d) 120-min powder

Figure 5. BEMs of sintered pellets (continued).

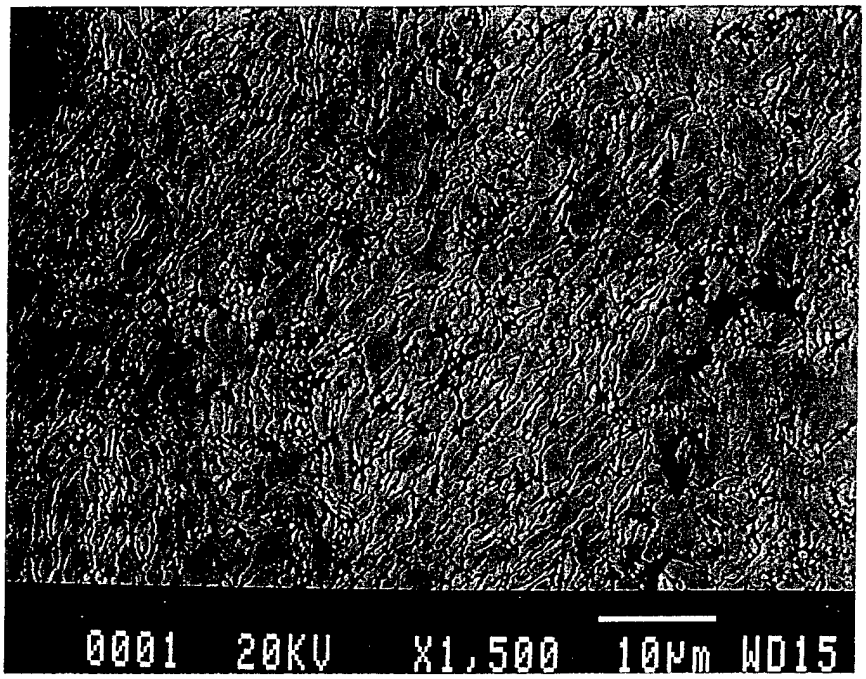

(e) 240-min powder

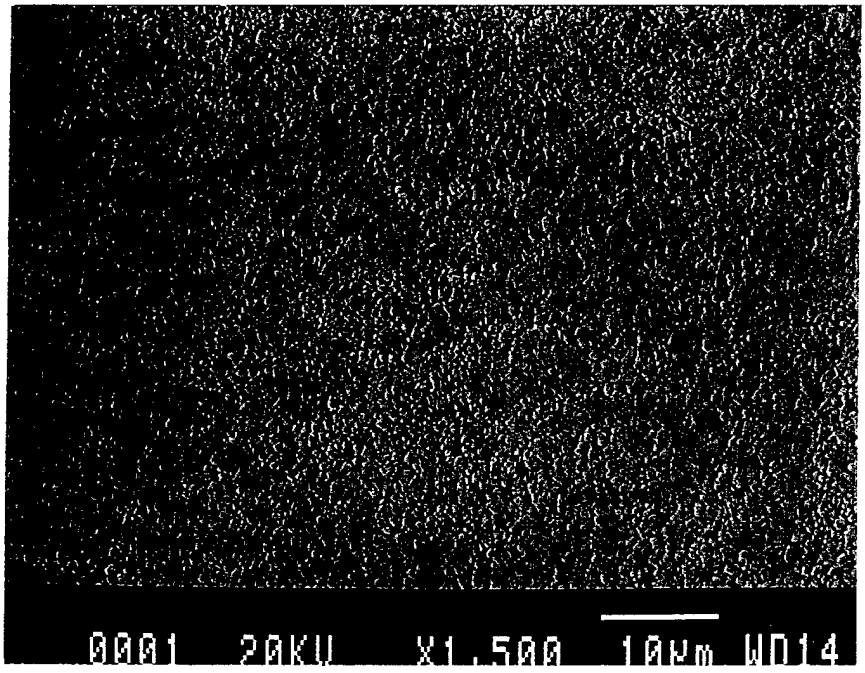

(f) 480-min powder

Figure 5. BEMs of sintered pellets (continued).

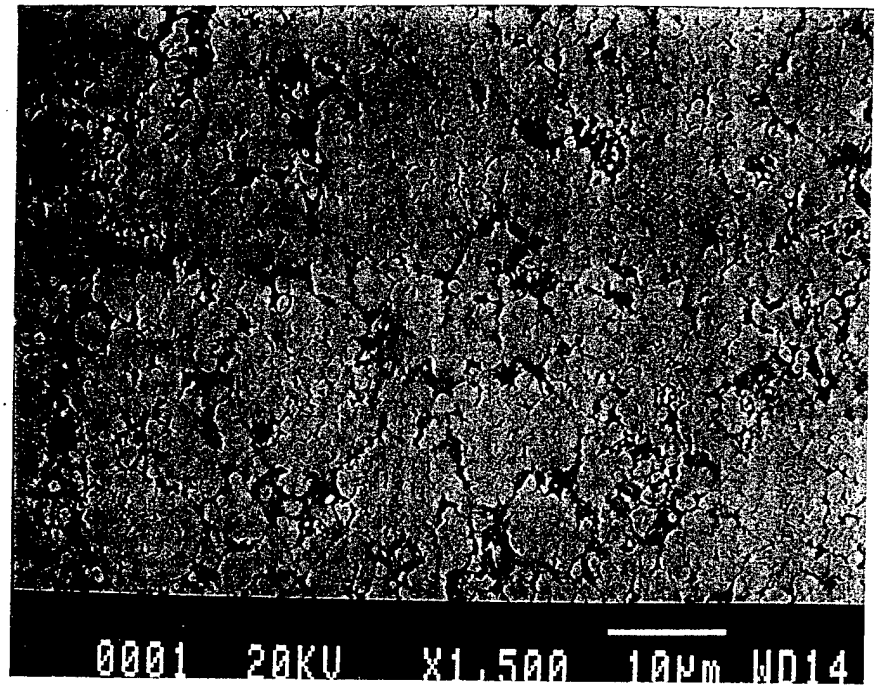

(g) 1,440-min powder

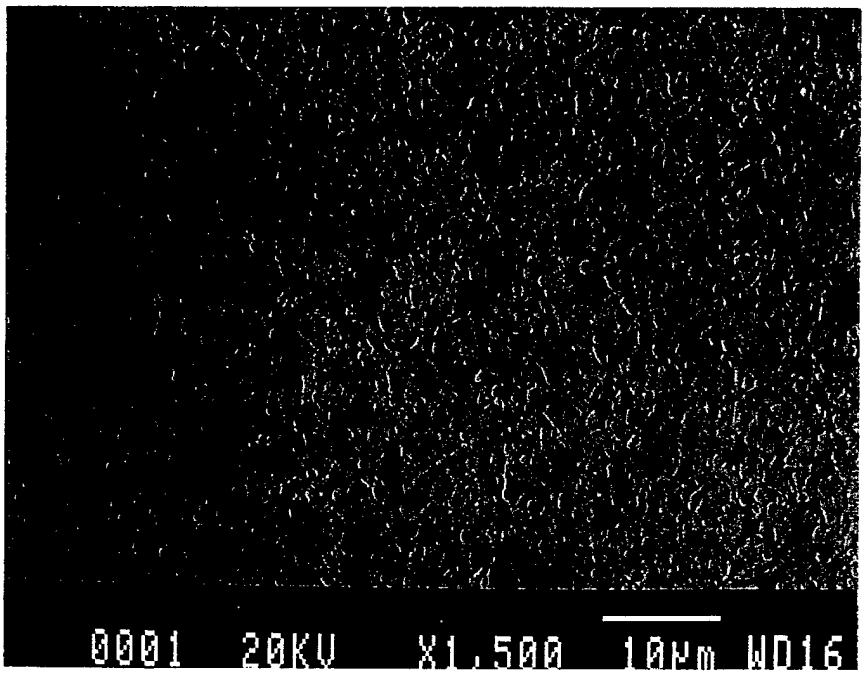

(h) 2,880-min powder

Figure 5. BEMs of sintered pellets (continued).

and/or balls, which is a common occurrence during ball milling. In contrast, the amounts of oxygen and carbon were about the same in both series B and C samples and were not found to vary with milling time, thereby negating the immediate benefits in using hexane for short milling times.

3.3 X-ray Diffraction Results

The characteristic patterns of the as-milled powders and the corresponding sintered pellets from series A are shown in Figures 6(a) through 6(d). The as-mixed baseline is included for reference. In both figures, the W and Cu peaks are clearly recognized. With longer milling times, the XRD patterns contain additional peaks. These peaks may be associated with the aluminum holder, Fe contamination from the mill, or oxides of W or Cu. All powder samples revealed extensive peak broadening with milling time. The observed peak broadening in Figure 6(a) arises from a combination of decreasing particle size and milling introduced lattice strain. Based on the expected theoretical line broadening (0.01° for 1-μm grain) caused by crystallite size reduction [10] and the actual refinement of the W grains, it is expected that beyond 480 min of milling, most of the broadening would be caused by lattice strain. Note that after the high-temperature sintering, the XRD patterns look essentially the same regardless of the milling time (Figures 6[c] and 6[d]).

The as-milled and post-sinter lattice parameters of W and Cu and the integrated Cu (200)/W(200) peak intensity ratios from series A are shown in Table 2 and Figures 7 and 8. Generally, with increasing milling time, there is a decreasing trend in the lattice parameters and relative peak ratios of W and Cu. XRD analyses of the as-milled powders and sintered samples from series B and C were consistent with the findings from series A (see Tables 3 and 4, as well as Figures 9 and 10). The data also indicated that the effect of milling in air or hexane on the lattice parameter was negligible over the milling times examined.

As shown in Figures 7(a) and 7(b), there is little change in the lattice parameters of Cu and W for milling times up to about 240 min. (The lattice parameters from the as-mixed powder do not appear on the logarithmic graphs.) At, and beyond, 240 min of milling, the as-milled W lattice parameter begins to decrease. There is a corresponding decrease for Cu. However, because of the considerable peak broadening, the drop is not so definitive. Recall, for Cu, the measurement error in the lattice parameters is considerably greater at long milling times. The actual change in the lattice parameter is only about a 0.5–1%; nevertheless, it is a clear indication of mechanical alloying [11]. As the respective lattice structures of W and Cu are being modified by milling, on an atomic scale, interdiffusion of W into Cu and Cu into W is occurring. A further, more important, aspect of the data is that after sintering, the decrease in the lattice parameters is absent.

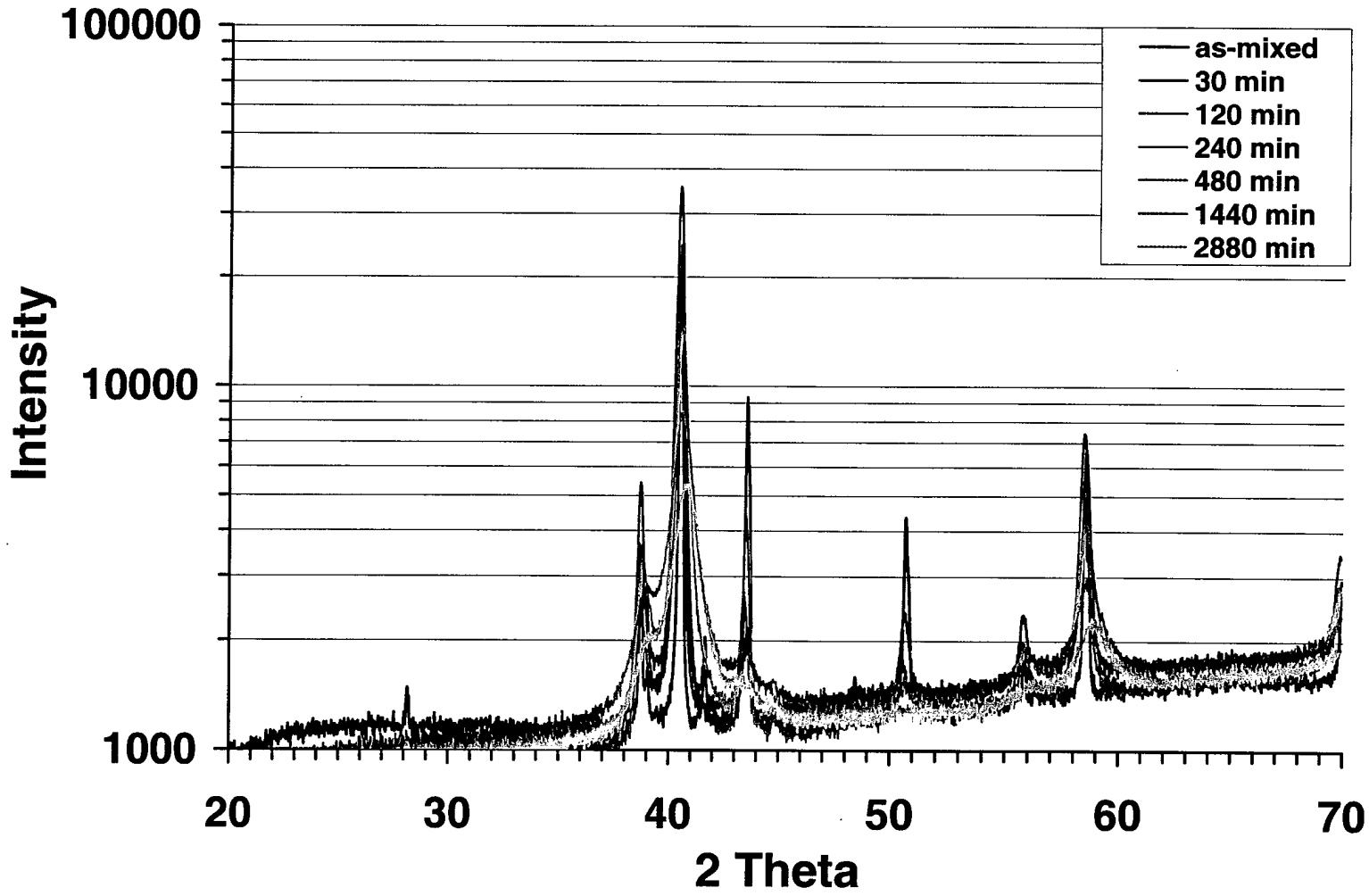

(a) as-milled powder; 20° to 70°

Figure 6. Selected XRD patterns of the W-Cu samples.

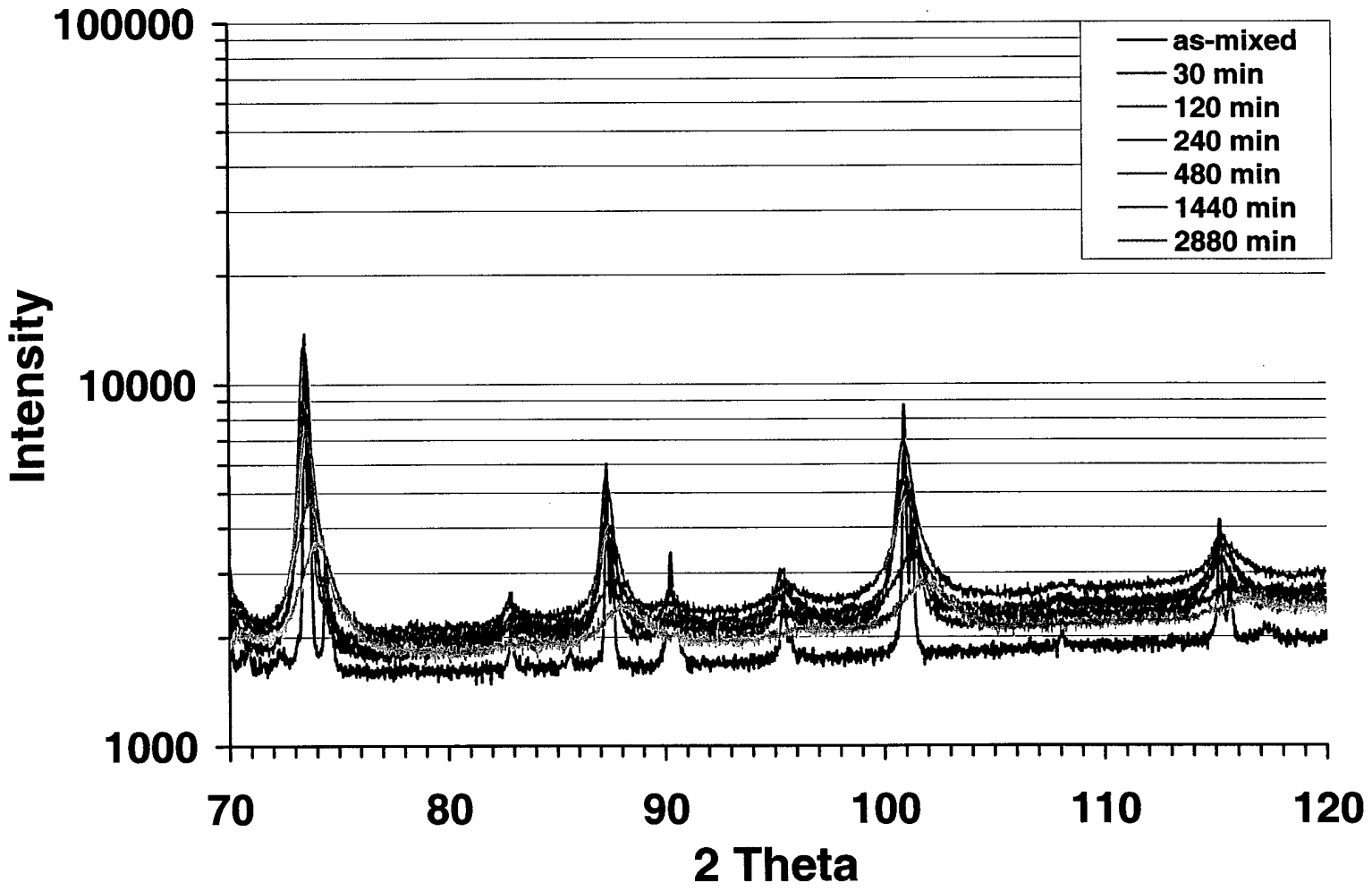

(b) as-milled powder; 70° to 120°

Figure 6. Selected XRD patterns of the W-Cu samples (continued).

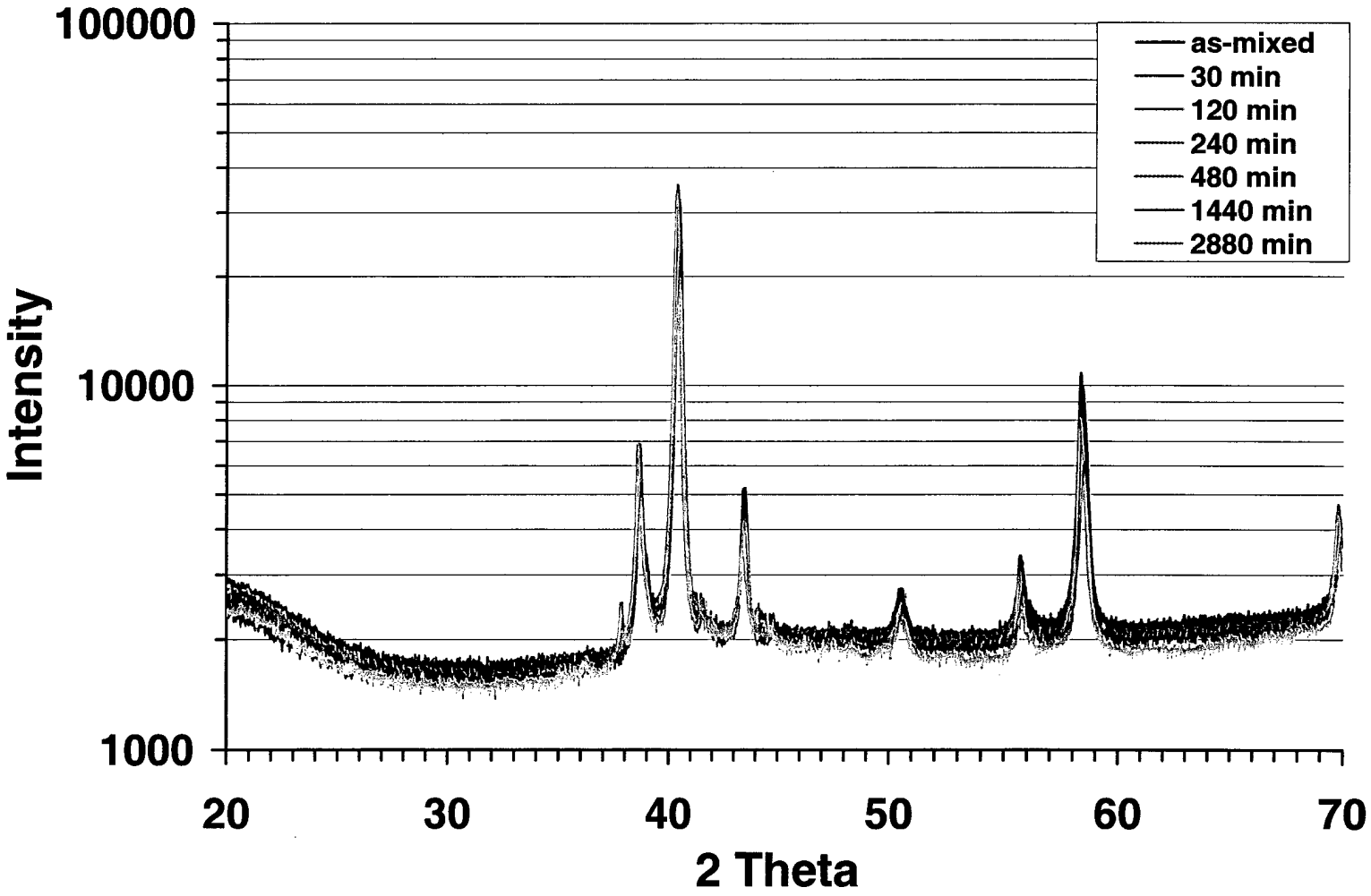

(c) sintered pellet; 20° to 70°

Figure 6. Selected XRD patterns of the W-Cu samples (continued).

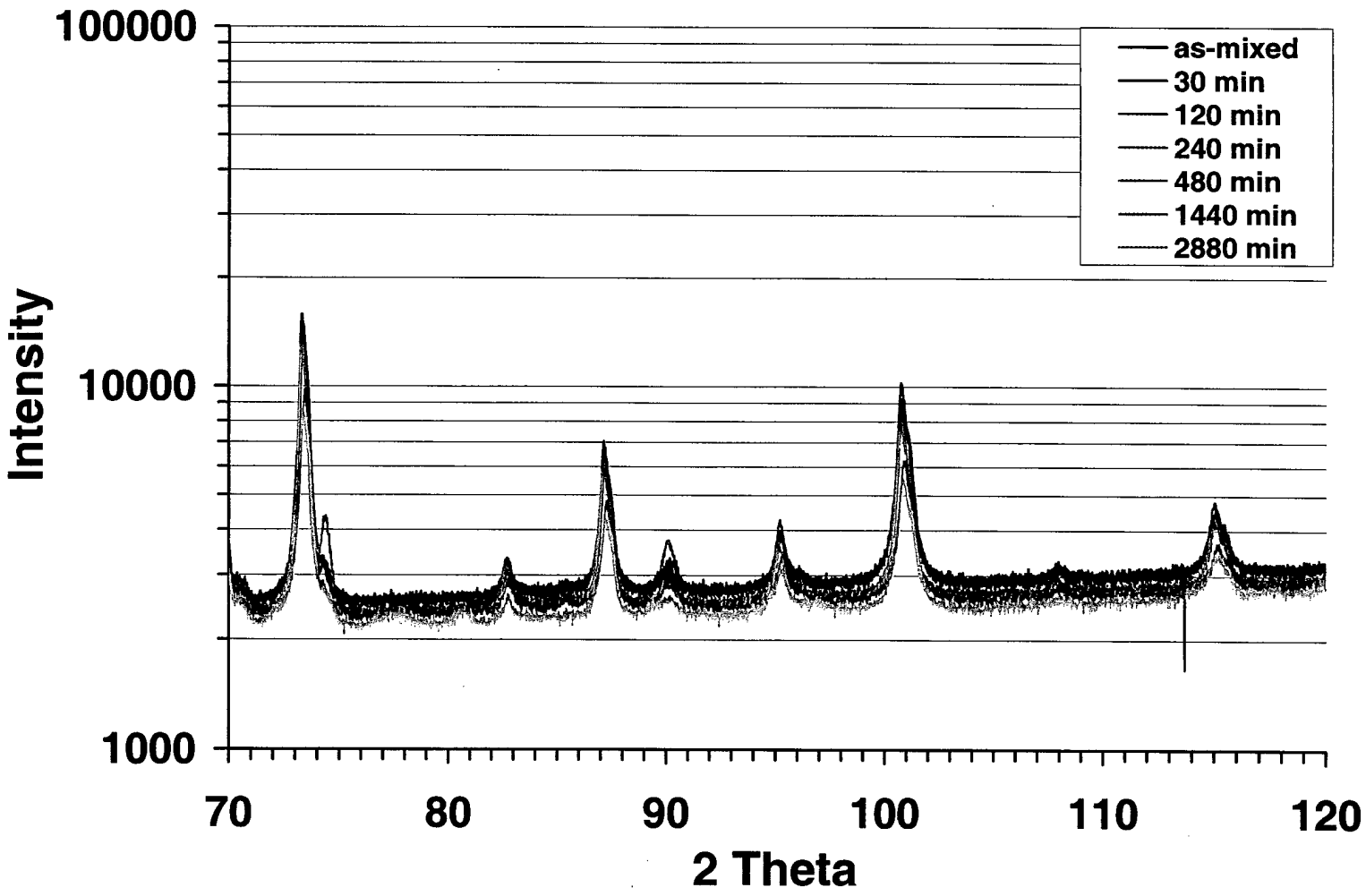

(d) sintered pellet; 70° to 120°

Figure 6. Selected XRD patterns of the W-Cu samples (continued).

Table 2. XRD results for series A; mixed in air.

Sample	Milling Time (min)	As-Milled Lattice Parameter (nm)		As-Milled Cu(200)/W(200) Peak Ratio	Post-Sintered Lattice Parameter (nm)		Post-Sintered Cu(200)/W(200) Peak Ratio
		W	Cu		W	Cu	
A1	0	0.3161	0.3610	0.76	0.3163	0.3614	0.11
A2	15	0.3162	0.3610	0.18	0.3163	0.3614	0.09
A3	30	0.3163	0.3610	0.13	0.3163	0.3613	0.07
A4	60	0.3164	0.3611	0.10	0.3162	0.3610	0.08
A5	120	0.3162	0.3610	0.09	0.3164	0.3612	0.07
A6	240	0.3162	0.3604	0.10	0.3163	0.3612	0.04
A7	480	0.3159	0.3603	0.03	0.3163	0.3615	0.06
A8	1,440	0.3155	0.3613	0.00	0.3160	0.3610	0.10
A9	2,880	0.3147	0.3590	0.00	0.3162	0.3609	0.14

From Figure 8, it is also apparent that the relative ratio of the integrated Cu and W peak heights varies as milling time increases, reflecting a relative shift in volume fractions of the constituents. The Cu(200)/W(200) peak ratio from the as-milled powder, which is a measure of the average volume ratio of the Cu and W phases, monotonically decreases with milling. This indicates that the "forced" diffusion of W into Cu and Cu into W is preferential. Specifically, Cu diffuses more readily into W than W into Cu. This is understandable, since, at the processing temperatures, the mobility of Cu would be considerably higher than that of W. However, as was found before, the initial Cu volume fraction is essentially recovered upon sintering.

While data from series A describe the effect of milling time, data from series D (the auxiliary experiment) demonstrate the effect of anneal temperature on the peak profile and lattice parameter. The results are tabulated in Table 5, with Figures 11 and 12 depicting the changes graphically. For W (Figure 11[a]), the lattice parameter relaxes at about 450 °C from an "alloyed" W-Cu state to an "unalloyed" pure W state. The transition occurs at a temperature slightly below one half of T_m of Cu. That is, above this temperature Cu is sufficiently mobile to diffuse out of the distorted W lattice, thereby allowing it to return to its initial, undeformed state. In contrast, as apparent in Figure 11[b], the extent of "reverse" alloying of W in Cu is considerably less than that of Cu in W. Note

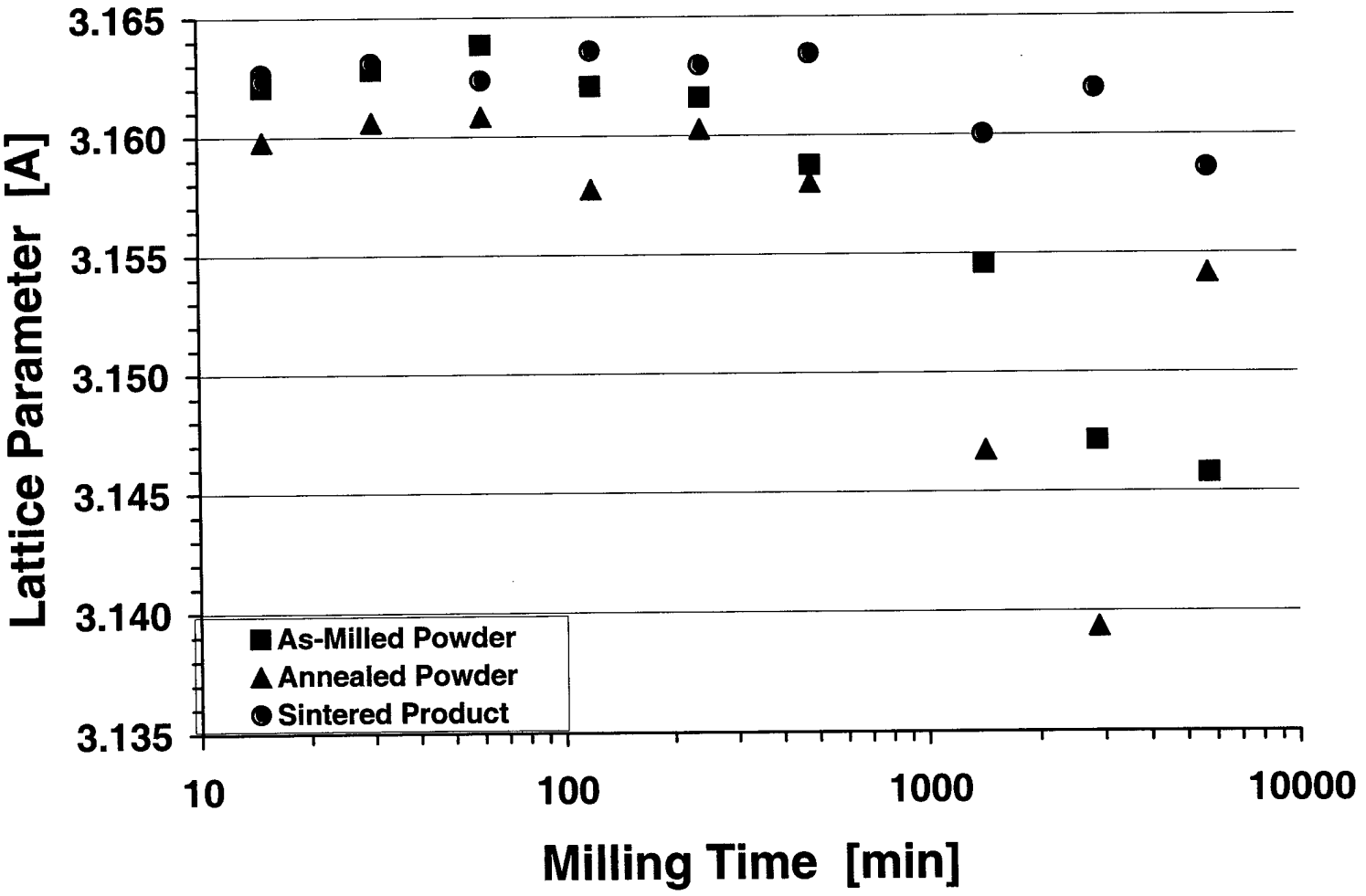

(a) W

Figure 7. Lattice parameters of the series A; air W-Cu samples.

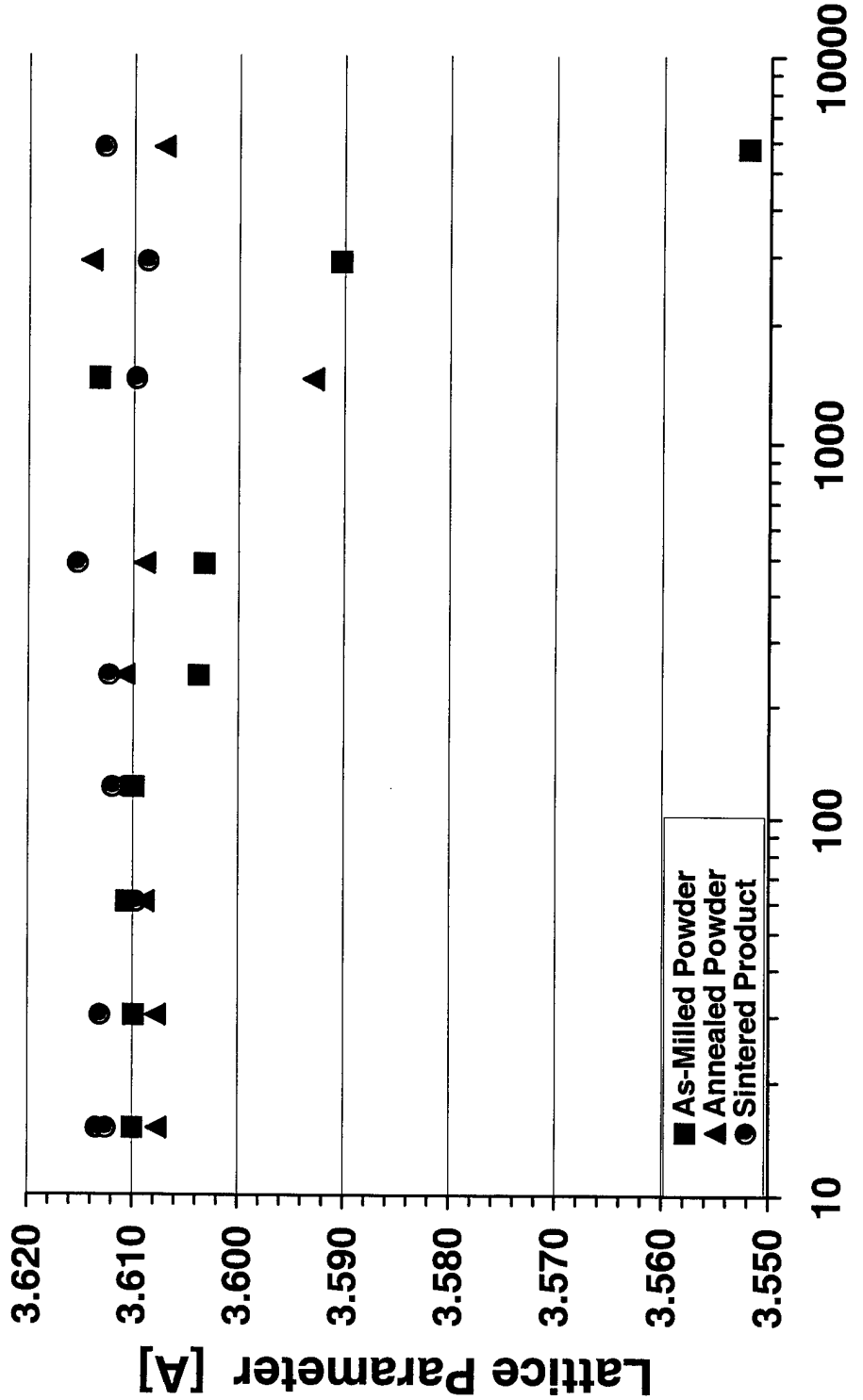

(b) Cu

Figure 7. Lattice parameters of the series A; air W-Cu samples (continued).

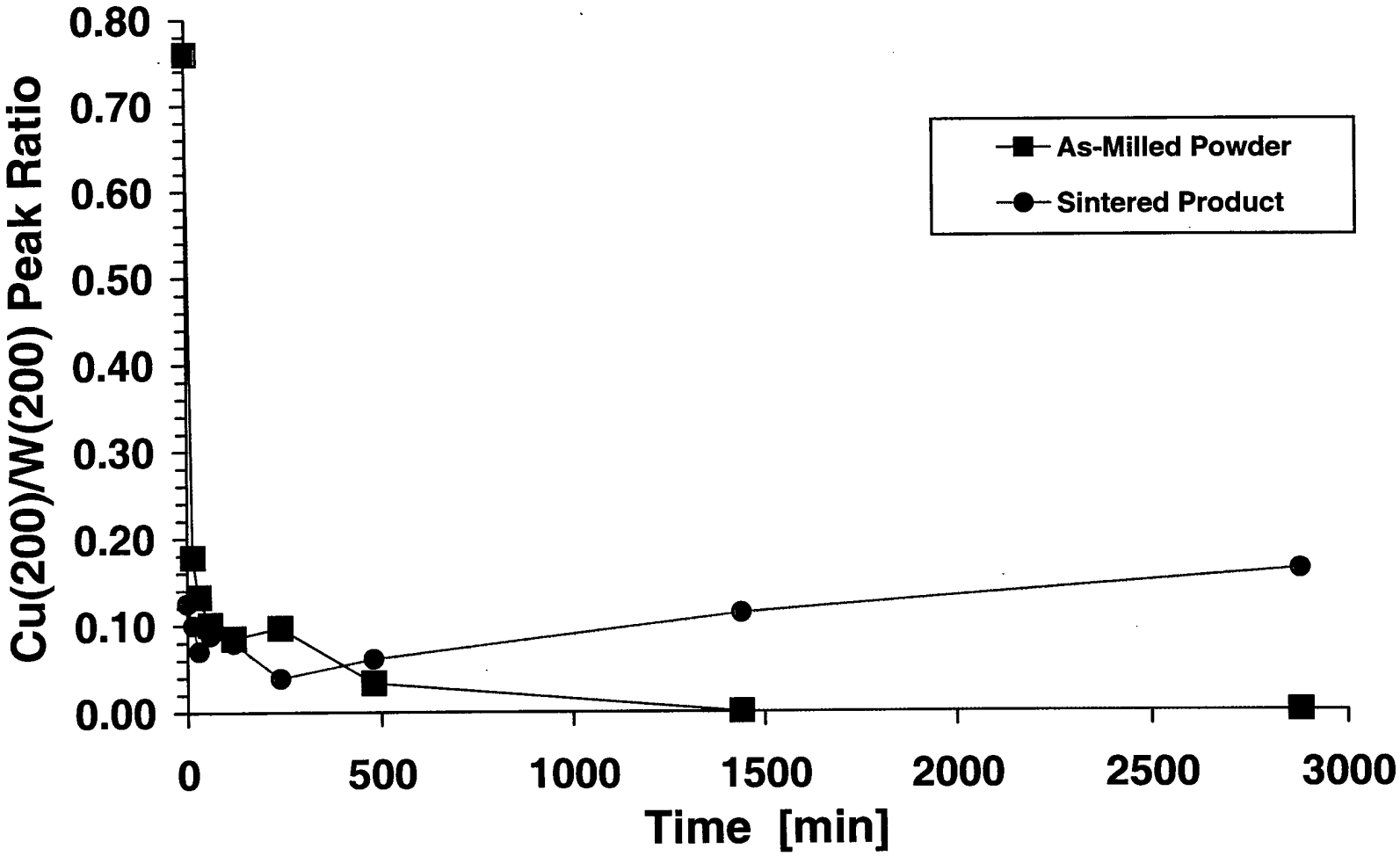

Figure 8. XRD W(200)/Cu(200) peak intensity ratio for the series A samples.

Table 3. XRD results for series B; mixed in air.

Sample	Milling Time (min)	As-Milled Lattice Parameter (nm)		As Milled Cu(200)/ W(200) Peak Ratio	Post-Sinter Lattice Parameter (nm)		Post-Sintered Cu(200)/ W(200) Peak Ratio
		W	Cu		W	Cu	
B1	120	0.3160	0.3606	0.15	0.3162	0.3612	0.14
B2	240	0.3161	0.3605	0.09	0.3162	0.3613	0.12
B3	480	0.3160	0.3610	0.09	0.3164	0.3610	0.06
B4	480	0.3159	0.3606	0.07	0.3164	0.3611	0.06
B5	1,440	0.3160	0.3591	0.03	0.3161	0.3612	0.22
B6	2,880	0.3156	0.3595	0.00	0.3163	0.3606	0.08

Table 4. XRD results for series C; mixed in hexane.

Sample	Milling Time (min)	As-Milled Lattice Parameter (nm)		As Milled Cu(200)/ W(200) Peak Ratio	Post-Sinter Lattice Parameter (nm)		Post-Sintered Cu(200)/ W(200) Peak Ratio
		W	Cu		W	Cu	
C1	120	0.3161	0.3608	0.24	0.3162	0.3614	0.11
C2	240	0.3160	0.3608	0.10	0.3162	0.3611	0.10
C3	240	0.3160	0.3603	0.17	0.3162	0.3611	0.14
C4	480	0.3163	0.3603	0.11	0.3162	0.3614	0.13
C5	480	0.3160	0.3607	0.07	0.3162	0.3608	0.09
C6	1,440	0.3163	0.3614	0.08	0.3162	0.3610	0.08
C7	2,880	0.3155	0.3615	0.01	0.3161	0.3611	0.06

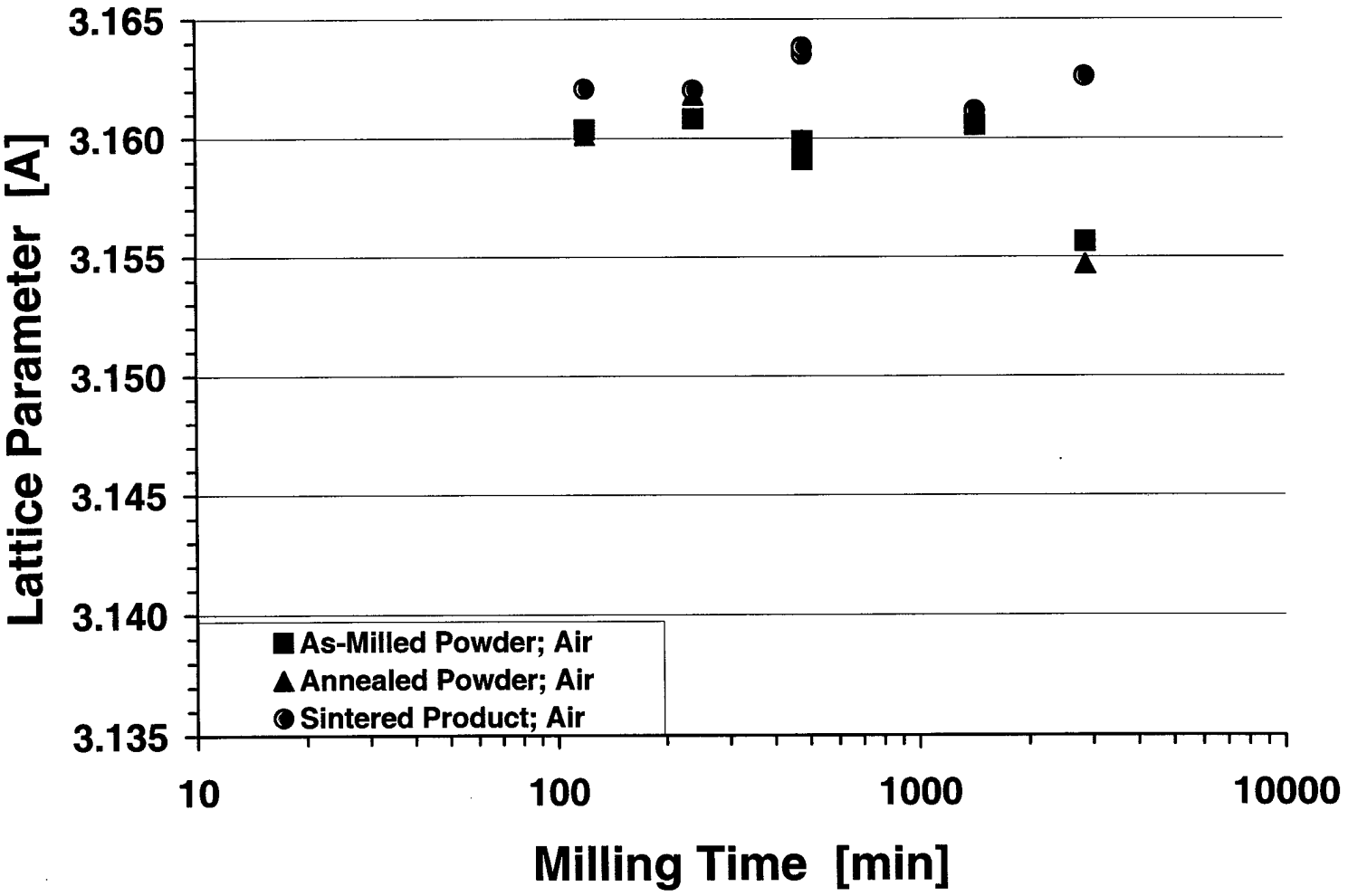

(a) W

Figure 9. Lattice parameters of the series B; air W-Cu samples.

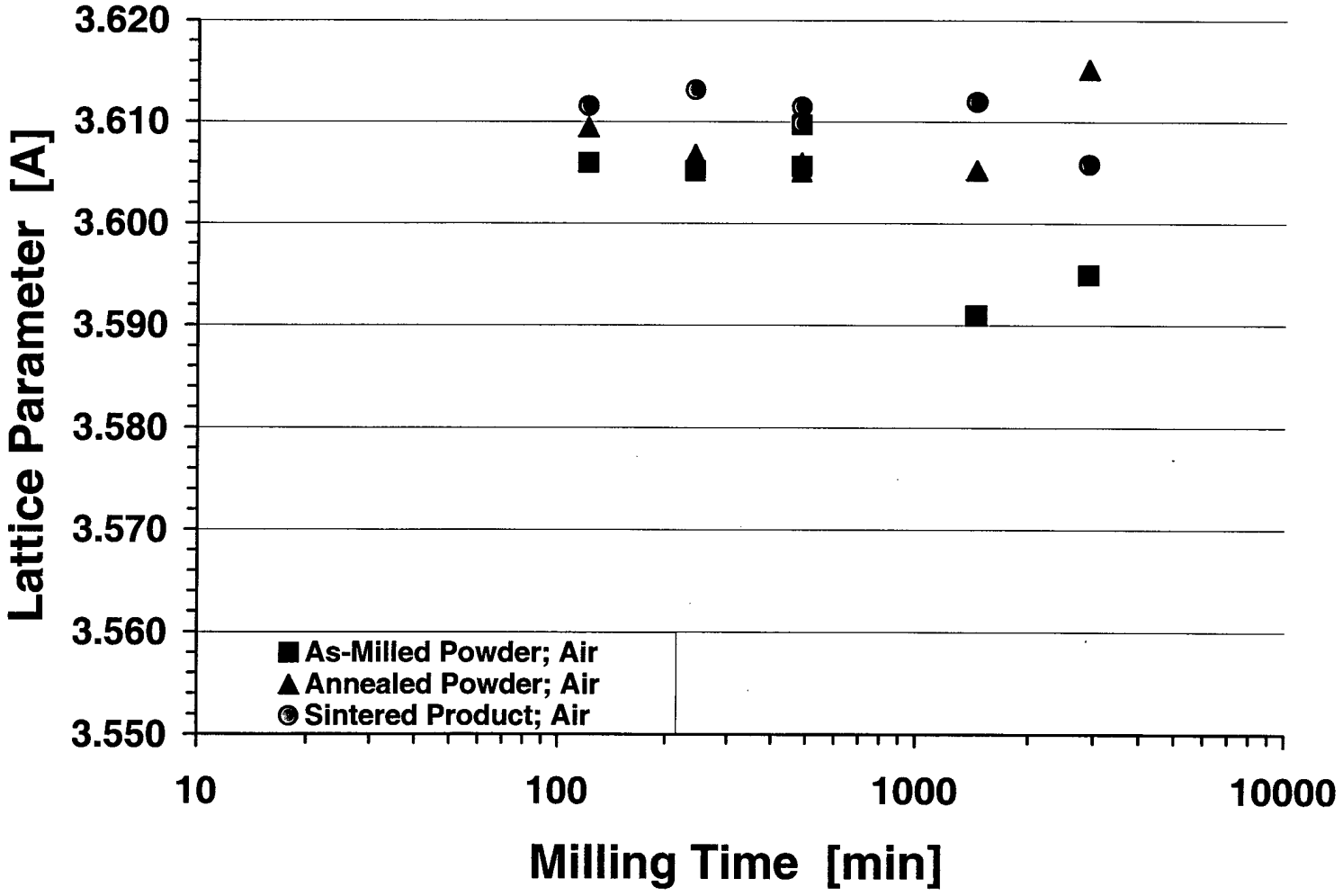

(b) Cu

Figure 9. Lattice parameters of the series B; air W-Cu samples (continued).

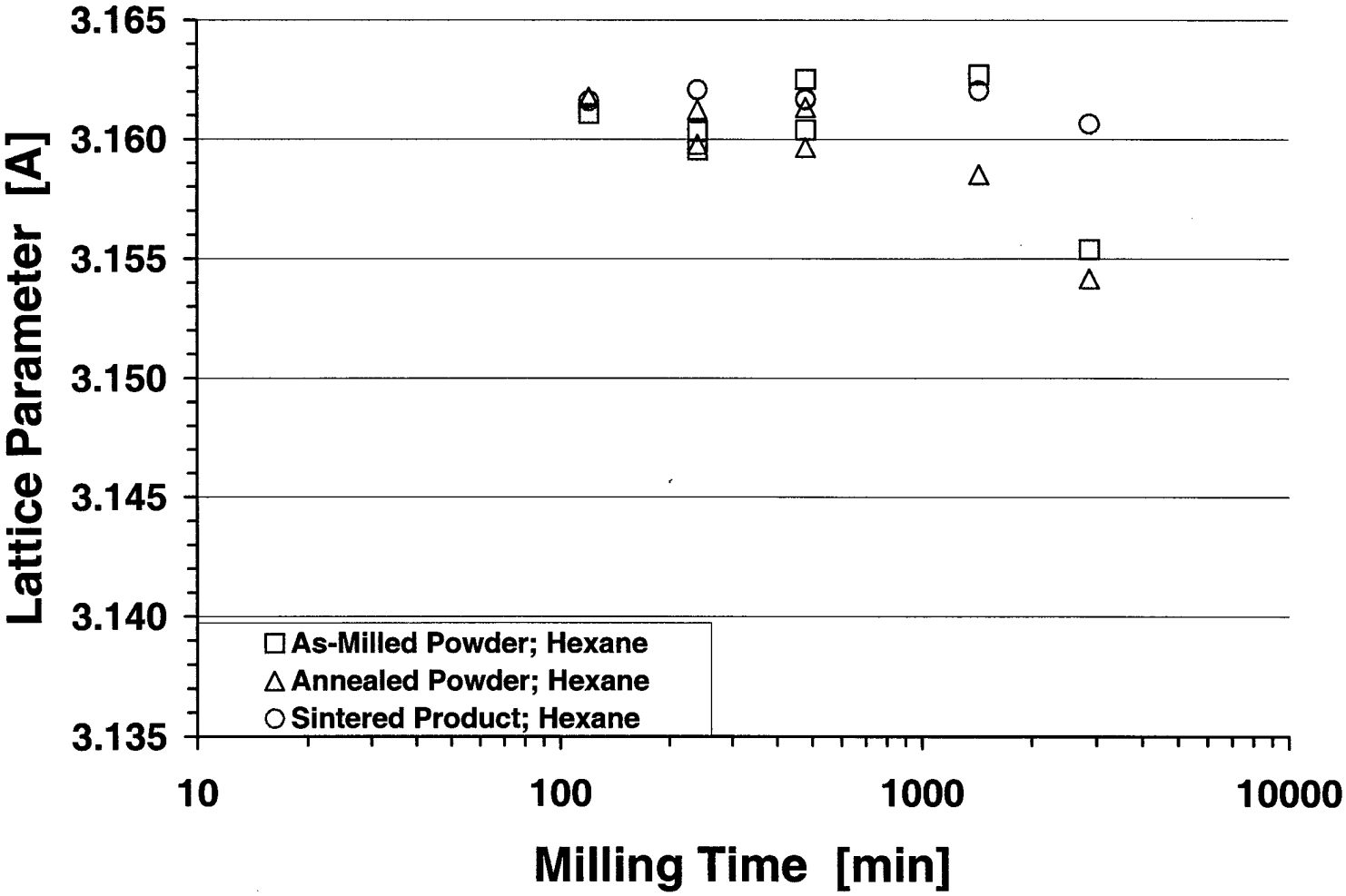

(a) W

Figure 10. Lattice parameters of the series C; hexane W-Cu samples.

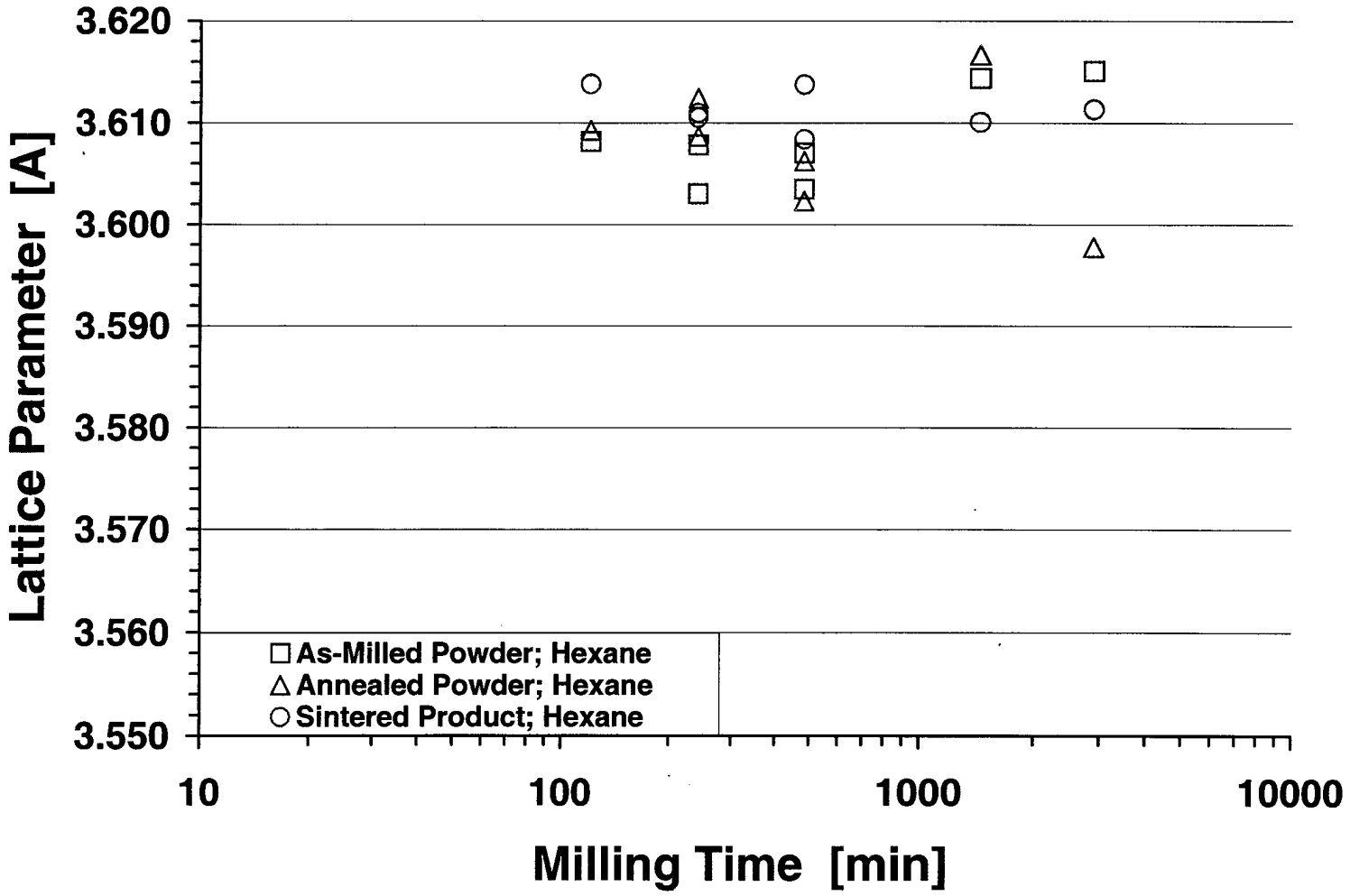

(b) Cu

Figure 10. Lattice parameters of the series C; hexane W-Cu samples (continued).

Table 5. XRD results for series D; mixed in air.

Sample	Anneal Temp (°C)	Density (%TD)	Micro-hardness 200-gf (GPa)	Post-Anneal Lattice Parameter (nm)		Post-Anneal 2θ-Peak Width (°)		Post-Sinter Lattice Parameter (nm)		Post-Sinter 2θ-Peak Width (°)	
				W	Cu	W(200)	Cu(200)	W	Cu	W(200)	Cu(200)
D1	–	94.9	3.48	0.3156	0.3606	0.59	0.31	0.3163	0.3609	0.34	0.21
D2	350	96.6	3.44	0.3156	0.3607	0.54	0.31	0.3163	0.3609	0.33	0.18
D3	450	96.7	3.33	0.3162	0.3608	0.52	0.25	0.3163	0.3609	0.36	0.26
D4	550	96.8	3.56	0.3160	0.3604	0.50	0.26	0.3162	0.3608	0.32	0.22
D5	650	97.3	3.54	0.3160	0.3611	0.48	0.23	0.3163	0.3609	0.36	0.29
D6	750	98.6	3.69	0.3159	0.3612	0.43	0.22	0.3163	0.3610	0.36	0.22
D7	850	95.0	3.20	0.3160	0.3611	0.39	0.19	0.3163	0.3610	0.36	0.20
D8	950	94.3	3.54	0.3161	0.3612	0.32	0.20	0.3162	0.3608	0.34	0.18

that the diffusion of the W atoms out of the Cu lattice occurs over a wider temperature range of about 350–550 °C.

Annealing prior to sintering was found to reduce the milling induced peak broadening as well. Results of the measurements of the full widths at half maximum (FWHM) of the W(200) and Cu(200) peaks are shown in Figure 12. Recall that the powders in series D were milled for 480 min only. This length of milling time introduces a considerable amount of strain into W; however, the corresponding amount of strain in Cu is significantly less. Most of the milling induced strain is gradually relieved by 950 °C in both of the "Cu-rich" W and "W-rich" Cu phases. Note in the figure that there is no further strain relief of either phase after sintering. Density measurements showed no gain in sample density; and, SEM examination of the sintered pellets did not reveal any considerable grain growth indicative of no improvement in sinterability after 480 min of milling.

The reduction in lattice parameters and their subsequent release on annealing and/or sintering may be explained as follows. Despite their mutual insolubility (or dislike for one another) during milling, both Cu and W atoms are progressively mechanically alloyed. Although the lattice structures of W and Cu are different (body-centered vs. face-centered cubic), the relative atomic radii (Cu: 0.128 nm; W: 0.138 nm) [12] are only 8% apart. Therefore, random atom-for-atom substitution is quite possible, forming metastable "Cu-rich" W and "W-rich" Cu solid solution regions. The small size difference between the respective

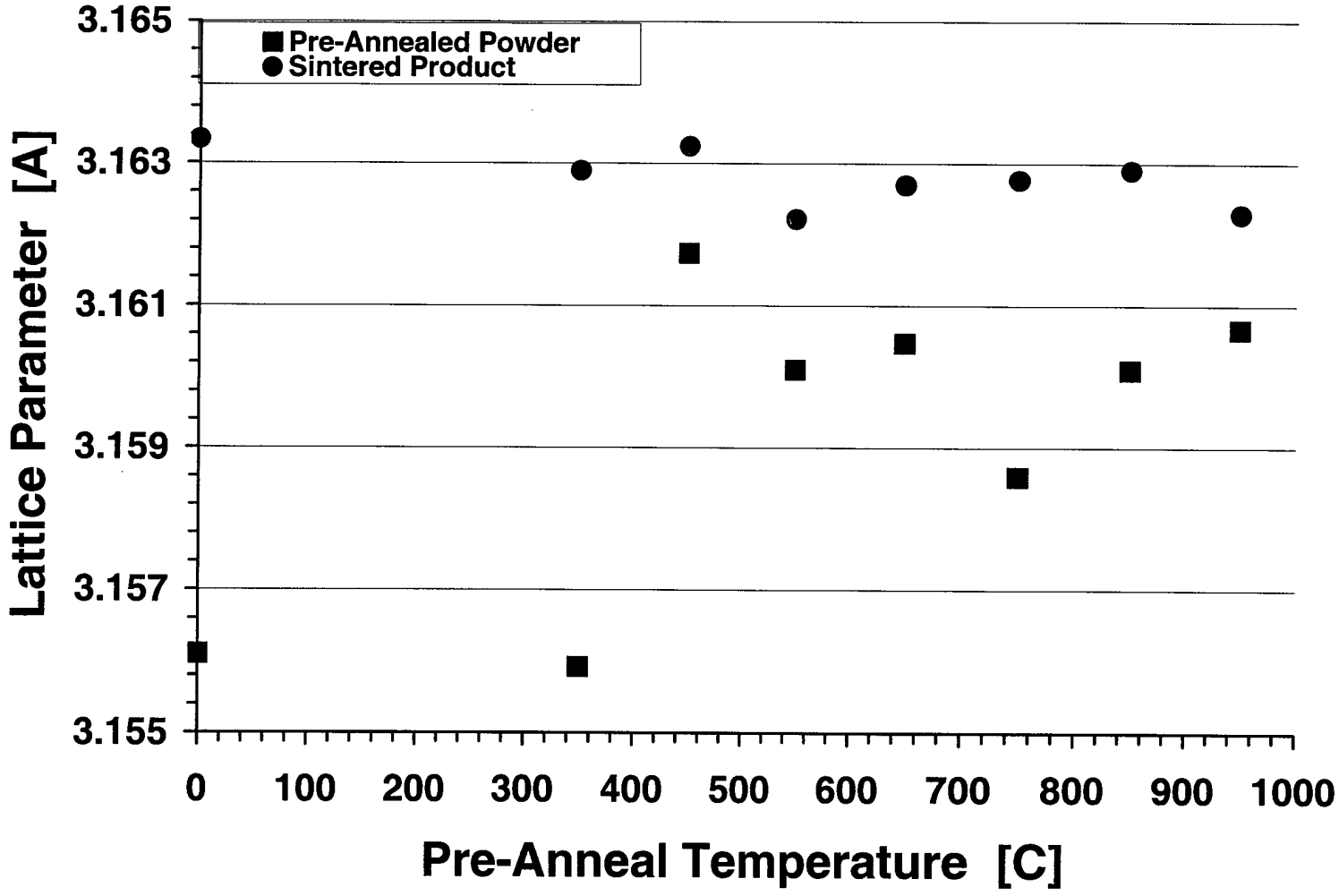

(a) W

Figure 11. Lattice parameters of the series D; anneal W-Cu samples.

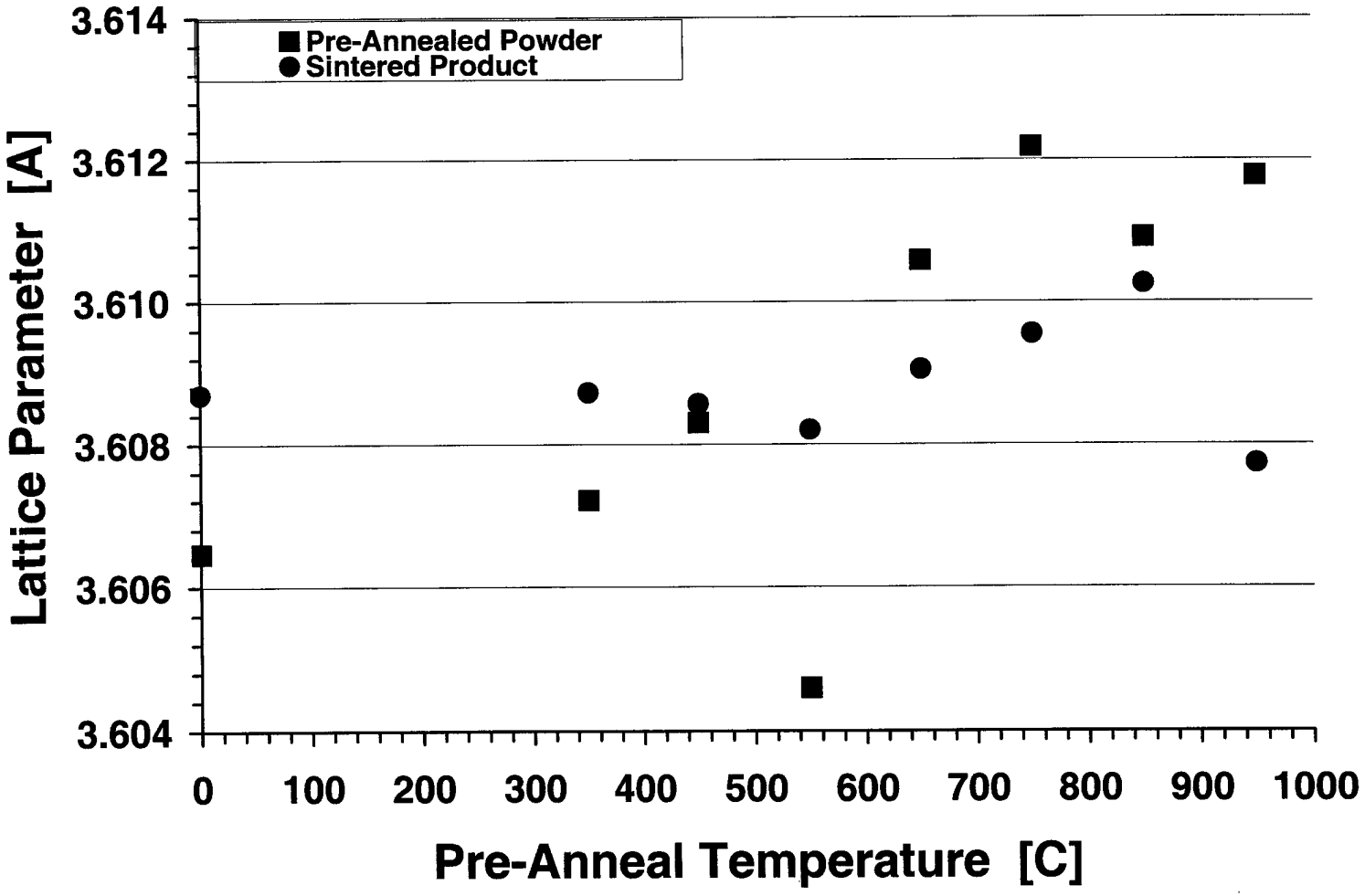

(b) Cu

Figure 11. Lattice parameters of the series D; anneal W-Cu samples (continued).

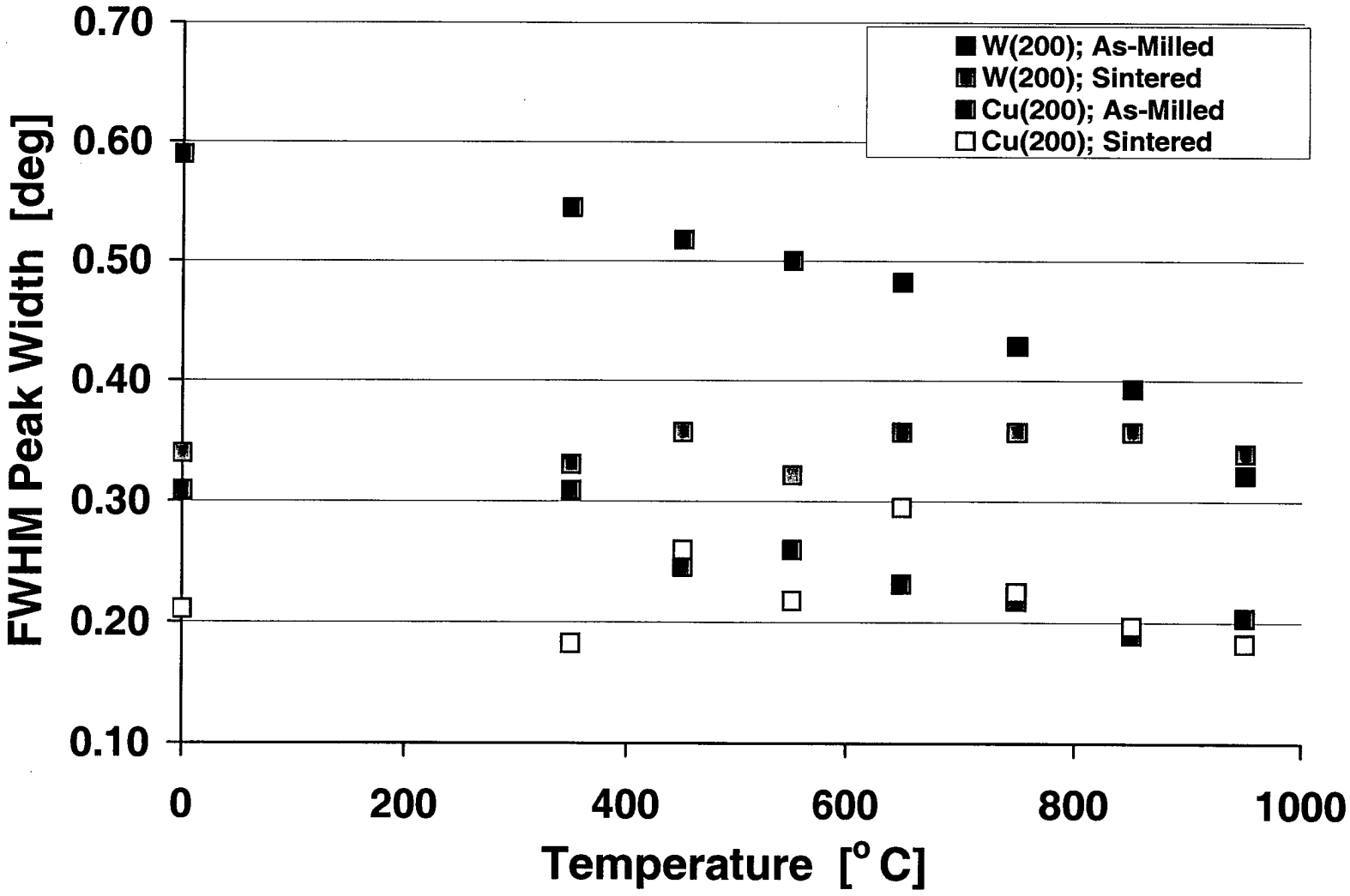

Figure 12. Post-anneal and post-sinter W(200) and Cu(200) peak widths for the series D.

atoms easily accounts for the observed decrease in the lattice dimensions or unit cell. At around 450 °C, the mobility of W is not very high; however, for Cu this is near the recrystallization temperature and, therefore, Cu would be fairly mobile. Then, the metastable, solid-solution regions would readily revert to their natural, segregated, thermodynamically-favored state. At higher temperatures, during annealing or sintering, the "Cu-rich" W and "W-rich" Cu solid solution regions decompose and segregate into "pure" Cu and "pure" W considerably faster. However, as soon as phase separation is completed, the immiscibility of Cu in W and W in Cu inhibits grain growth or coarsening, and the overall structure is preserved.

3.4 Microhardness Results

Based on the microhardness results displayed in Table 1, it may be surmised that the mechanically alloyed and sintered samples from all three series primarily show the effects of dispersion and solid-solution hardening with milling time. The hardness results appeared to be essentially independent of the milling medium used (Figure 13). At short milling times, the low hardness values correspond to the two macroscopically distinct phases in the samples as well as trapped porosity. However, at longer times, as the grain size is reduced, W and Cu are better dispersed, and densification improves, the hardness increases dramatically by over a factor of two. The drop in hardness of the samples at 2,880 min is probably caused by either higher residual porosity levels (grain coarsening) or intergrain embrittlement (impurity segregation).

4. Summary and Conclusions

Mechanical alloying of 80W-20Cu was achieved by ball-milling W and Cu mixtures in air, followed by LPS above the T_m of Cu. Near-full densification was achieved after 480 min of milling. After milling, the initially 2-5 μm polyhedral W grains broke down and the product morphology was fine-grained and equiaxed; the average W grain size was reduced by an order-of-magnitude to about 0.2–0.5 μm. Longer milling did not reduce the W grain size any further. Lattice parameter and line broadening analyses confirmed the presence of metastable "W-rich" Cu and "Cu-rich" W phases. That is, W and Cu were being mechanically alloyed at a submicrometer level. However, due to the thermodynamically favored phase separation at the sintering temperature, the resultant composites consisted of submicrometer W grains surrounded by a Cu matrix. The onset of this phase separation was found to occur at a low temperature of about 450 °C. The reversion of the alloyed structure into its immiscible constituents also diminished the sinterability of the powders, thereby mostly retaining the as-milled grain size.

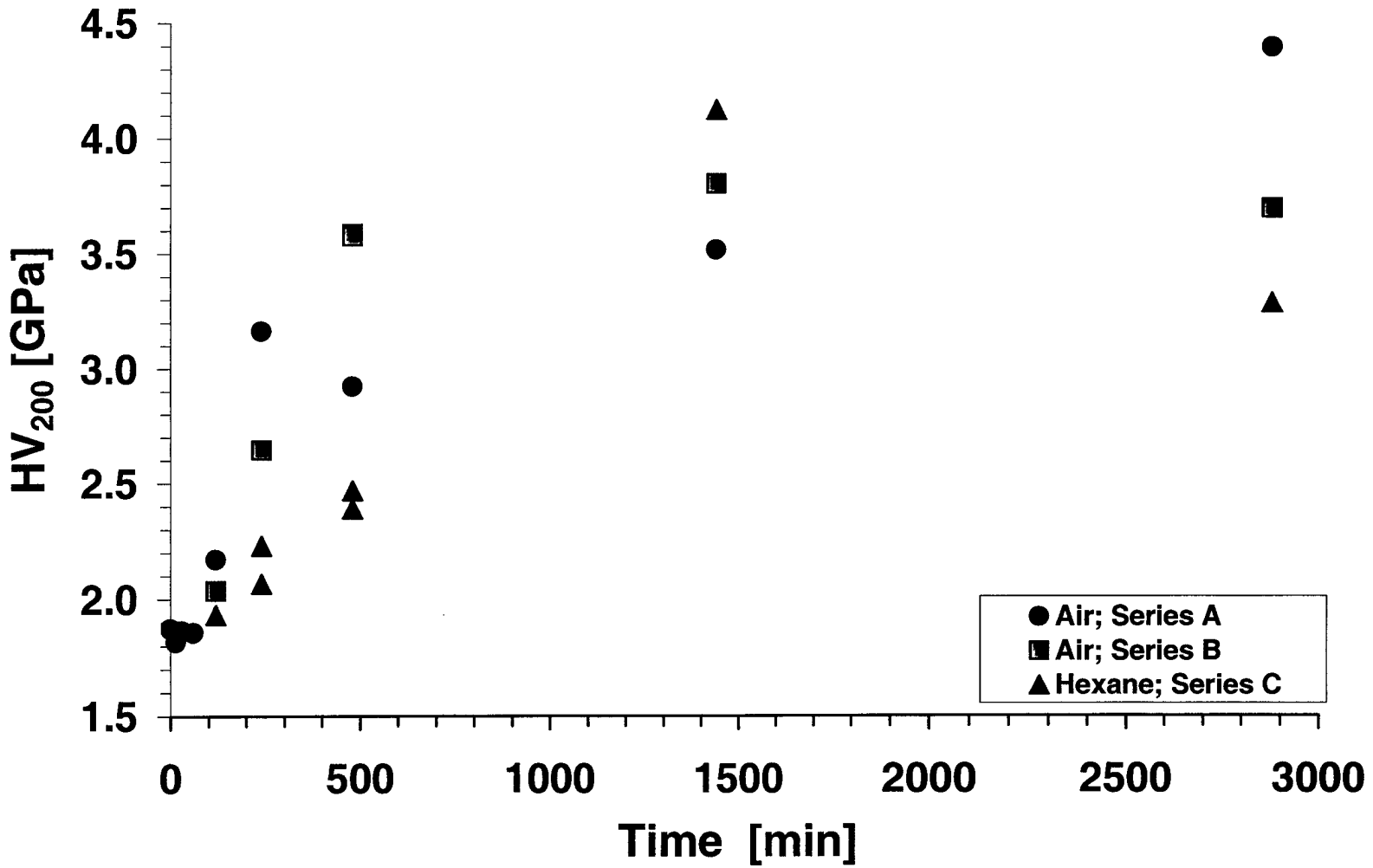

Figure 13. W-Cu sample microhardness as a function of milling time.

While the use of hexane as a milling medium was possibly beneficial in reducing impurity pick-up from the milling media and environment, densification and the rate of intermixing or alloying of the precursors were retarded. Only the sample milled in hexane for 2,880 min reached full density. EDS measurements indicated that the as-milled powders and sintered pellets were highly sensitive to contamination during extended periods of milling as impurity levels increased with increasing milling times.

It is recommended that in order to produce full-density 80W-20Cu composites, longer milling times in hexane will be necessary. Furthermore, the duration of sintering could be also extended. However, in order to reduce contamination, experiments ought to be performed with powder-to-ball mass ratios of about 1:10. By using lower ratios, the effects of milling would not only be further enhanced, but also yield faster results in shorter milling times.

INTENTIONALLY LEFT BLANK.

5. References

1. Bose, A., and R. M. German. "Developments in the Sintering of Tungsten Heavy Alloys." *Sintering Theory and Practice.* New York, NY: John Wiley & Sons, Inc., 1996.

2. German, R. M., K. F. Hens, J. L. Johnson, and Y. Bin. "Powder Metallurgy Processing of Heat Dissipation Components for Microelectronic Applications." *Advances in Powder Metallurgy and Particulate Materials. Specialty Materials and Composites. Proceedings of the 1993 International Conference on Powder Metallurgy and Particulate Materials,* Princeton, NJ: MPIF Press, pp. 189–202, 1993.

3. Boscary, J., S. Suzuki, K. Nakamura, T. Suzuki, and M. Akiba. "Thermal Fatigue Tests on CVD-W/Cu Divertor Plates." *Proceedings of the 1997 Fourth*[h] *International Symposium on Fusion Nuclear Technology,* vol. 39–40, part A, Lausanne, Switzerland: Elsevier, pp. 537–542, 1999.

4. Massalski, T. B., H. Okamoto, P. R. Subramanian, and L. Kacprzak (editors). *Binary Alloy Phase Diagrams.* 2nd edition, New York, NY: William W. Scott Publishers, pp. 1503–1504, 1990.

5. Lee, G. G., G. H. Ha, D. W. Lee, B. K. Kim, and I. S. Ahn. "Synthesis of W/Cu Composite Alloys by Thermochemical Method." *TMS Annual Meeting Chemistry and Physics of Nanostructures and Related Non-Equilibrium Materials. Proceedings of the 1997 TMS Annual Meeting,* Warrendale, PA: TMS Society Press, pp. 163–170, 1997.

6. Ryu, H. J., S. H. Hong, J. W. Noh, and W. H. Baek. "Microstructure and Properties of Mechanically Alloyed Tungsten Heavy Alloy." *Second International Symposium on Advanced PM Processing (ISAPM-2),* Pohang, Korea, pp. 196–203, 1996.

7. Ovecoglu, M. L., and B. Ozkal. "Comparison of the Sintering Characteristics of Ball-Milled and Attritor-Milled W-Ni-Fe Heavy Alloy." *Journal of Materials Research,* vol. 11, no. 7, pp. 1673–1682, 1996.

8. Kim, J. C., and I. H. Moon. "Sintering of Nanostructured W-Cu Alloys Prepared by Mechanically Alloying." *Nanostructured Materials,* vol. 10, no. 2, pp. 283–290, 1998.

9. Upadhyaya, A., and R. M. German. "Densification and Dilation of Sintering W-Cu Alloys." *International Journal of Powdered Metallurgy,* vol. 34, no. 2, pp. 43–55, 1998.

10. Cullity, B. D. *Elements of X-ray Diffraction.* 2d ed., Reading, MA: Addison Wesley Publishing Company, Inc., pp. 359–360, 1978.

11. Gaffet, E., C. Louison, M. Harmelin, and F. Faudot. "Metastable Phase Transformations Induced by Ball Milling in the Cu-W System." *Materials Science and Engineering,* vol. A134, pp. 1380–1384, 1991.

12. Askeland, D. R. *The Science and Engineering of Materials.* 2nd ed., Boston, MA: PWS-Kent Publishing Company, p. 686, 1989.

NO. OF COPIES	ORGANIZATION
2	DEFENSE TECHNICAL INFORMATION CENTER DTIC OCA 8725 JOHN J KINGMAN RD STE 0944 FT BELVOIR VA 22060-6218
1	HQDA DAMO FDT 400 ARMY PENTAGON WASHINGTON DC 20310-0460
1	OSD OUSD(A&T)/ODDR&E(R) DR R J TREW 3800 DEFENSE PENTAGON WASHINGTON DC 20301-3800
1	COMMANDING GENERAL US ARMY MATERIEL CMD AMCRDA TF 5001 EISENHOWER AVE ALEXANDRIA VA 22333-0001
1	INST FOR ADVNCD TCHNLGY THE UNIV OF TEXAS AT AUSTIN 3925 W BRAKER LN STE 400 AUSTIN TX 78759-5316
1	DARPA SPECIAL PROJECTS OFFICE J CARLINI 3701 N FAIRFAX DR ARLINGTON VA 22203-1714
1	US MILITARY ACADEMY MATH SCI CTR EXCELLENCE MADN MATH MAJ HUBER THAYER HALL WEST POINT NY 10996-1786
1	DIRECTOR US ARMY RESEARCH LAB AMSRL D DR D SMITH 2800 POWDER MILL RD ADELPHI MD 20783-1197

NO. OF COPIES	ORGANIZATION
1	DIRECTOR US ARMY RESEARCH LAB AMSRL CI AI R 2800 POWDER MILL RD ADELPHI MD 20783-1197
3	DIRECTOR US ARMY RESEARCH LAB AMSRL CI LL 2800 POWDER MILL RD ADELPHI MD 20783-1197
3	DIRECTOR US ARMY RESEARCH LAB AMSRL CI AP 2800 POWDER MILL RD ADELPHI MD 20783-1197
	ABERDEEN PROVING GROUND
2	DIR USARL AMSRL CI LP (BLDG 305)

NO. OF COPIES	ORGANIZATION
1	HQDA SARD TR WASHINGTON DC 20301
1	CDR US ARMY RSCH OFC PO BOX 12211 RTP NC 27709-2211
1	CDR US ARMY ARDEC SMCAR TDC PICATINNY ARSENAL NJ 07801-5000
1	DIR BENET LABS SMCAR CCB TL WATERVLIET NY 12189
1	CDR US ARMY AMCCOM SMCAR ESP L ROCK ISLAND IL 61299
1	CDR US ARMY FOREIGN SCIENCE AND TECHNICAL CTR 220 SEVENTH ST NE CHARLOTTESVILLE VA 22901
1	GEORGIA INSTITUTE OF TECHNOLOGY MATERIALS SCIENCE & ENGINEERING M TREXLER 771 FERST DRIVE NW ATLANTA, GA 30332

NO. OF COPIES	ORGANIZATION
	ABERDEEN PROVING GROUND
39	DIR ARL R WHALIN J ROCCHIO AMSRL WM M D VIECHNICKI G HAGNAUER J MACAULEY J BEATTY B FINK W ROY R SHUFORD AMSRL WM T B BURNS A CARDAMONE W WALTERS L MAGNESS G BOYCE AMSRL WM MC J ADAMS E CHIN M STAKER AMSRL WM MD K ANDERSON K CHO W DE ROSSETT R DOWDING B GERSTEN L KECSKES (15 CPS) B KLOTZ D SNOHA

REPORT DOCUMENTATION PAGE

Form Approved
OMB No. 0704-0188

1. AGENCY USE ONLY *(Leave blank)*	2. REPORT DATE	3. REPORT TYPE AND DATES COVERED
	April 2001	Final, June 1998–August 2000

4. TITLE AND SUBTITLE
Mechanical Alloying Effects in Ball-Milled Tungsten-Copper (W-Cu) Composites

5. FUNDING NUMBERS
1L622105AH84622105A

6. AUTHOR(S)
Laszlo J. Kecskes, Matthew D. Trexler, Bradley R. Klotz, Kyu C. Cho, and Robert J. Dowding

7. PERFORMING ORGANIZATION NAME(S) AND ADDRESS(ES)
U.S. Army Research Laboratory
ATTN: AMSRL-WM-MD
Aberdeen Proving Ground, MD 21005-5069

8. PERFORMING ORGANIZATION REPORT NUMBER
ARL-TR-2465

9. SPONSORING/MONITORING AGENCY NAMES(S) AND ADDRESS(ES)

10.SPONSORING/MONITORING AGENCY REPORT NUMBER

11. SUPPLEMENTARY NOTES

12a. DISTRIBUTION/AVAILABILITY STATEMENT
Approved for public release; distribution is unlimited.

12b. DISTRIBUTION CODE

13. ABSTRACT *(Maximum 200 words)*

Fine-grained, high-density (97%+ of theoretical density [TD]), 80 tungsten-20 copper weight-percent (80W-20Cu [58W-42Cu atomic-percent]) composites have been prepared using nonconventional alloying techniques. The W and Cu precursor powders were combined by high-energy ball milling in air. A second set of W+Cu mixtures was prepared in hexane to reduce contamination of the powders. The mechanically alloyed W+Cu powder mixtures were then coldpressed into green compacts and sintered at 1,250 °C. The effects of varying the milling medium and milling time were examined with density measurements. Longer milling increased product densities with a concomitant order-of-magnitude decrease in grain size; air was found to be a more effective medium than hexane. Residual impurities were identified with energy-dispersive x-ray spectroscopy (EDS), and their effects on sample properties were evaluated with microhardness measurements. X-ray diffraction (XRD) and scanning electron microscopy (SEM) analyses demonstrated that the as-milled W-Cu alloy structures were metastable, decomposing into the starting W and Cu components upon heating at or above 450 °C.

14. SUBJECT TERMS
mechanical alloying, ball milling microstructure, tungsten, copper, metastable phases, x-ray diffraction, scanning electron microscopy, morphology, densification, microhardness, sintering

15. NUMBER OF PAGES
52

16. PRICE CODE

17. SECURITY CLASSIFICATION OF REPORT	18. SECURITY CLASSIFICATION OF THIS PAGE	19. SECURITY CLASSIFICATION OF ABSTRACT	20. LIMITATION OF ABSTRACT
UNCLASSIFIED	UNCLASSIFIED	UNCLASSIFIED	UL

INTENTIONALLY LEFT BLANK.

USER EVALUATION SHEET/CHANGE OF ADDRESS

This Laboratory undertakes a continuing effort to improve the quality of the reports it publishes. Your comments/answers to the items/questions below will aid us in our efforts.

1. ARL Report Number/Author ARL-TR-2465 (Kecskes) Date of Report April 2001

2. Date Report Received _____

3. Does this report satisfy a need? (Comment on purpose, related project, or other area of interest for which the report will be used.) _____

4. Specifically, how is the report being used? (Information source, design data, procedure, source of ideas, etc.) _____

5. Has the information in this report led to any quantitative savings as far as man-hours or dollars saved, operating costs avoided, or efficiencies achieved, etc? If so, please elaborate. _____

6. General Comments. What do you think should be changed to improve future reports? (Indicate changes to organization, technical content, format, etc.) _____

CURRENT ADDRESS

_____
Organization

_____
Name E-mail Name

_____
Street or P.O. Box No.

_____
City, State, Zip Code

7. If indicating a Change of Address or Address Correction, please provide the Current or Correct address above and the Old or Incorrect address below.

OLD ADDRESS

_____
Organization

_____
Name

_____
Street or P.O. Box No.

_____
City, State, Zip Code

(Remove this sheet, fold as indicated, tape closed, and mail.)
(DO NOT STAPLE)

DEPARTMENT OF THE ARMY

OFFICIAL BUSINESS

NO POSTAGE
NECESSARY
IF MAILED
IN THE
UNITED STATES

BUSINESS REPLY MAIL
FIRST CLASS PERMIT NO 0001,APG,MD

POSTAGE WILL BE PAID BY ADDRESSEE

DIRECTOR
US ARMY RESEARCH LABORATORY
ATTN AMSRL WM MD
ABERDEEN PROVING GROUND MD 21005-5066